

**Manuscript version: Author's Accepted Manuscript**

The version presented in WRAP is the author's accepted manuscript and may differ from the published version or Version of Record.

**Persistent WRAP URL:**

<http://wrap.warwick.ac.uk/107924>

**How to cite:**

Please refer to published version for the most recent bibliographic citation information. If a published version is known of, the repository item page linked to above, will contain details on accessing it.

**Copyright and reuse:**

The Warwick Research Archive Portal (WRAP) makes this work by researchers of the University of Warwick available open access under the following conditions.

Copyright © and all moral rights to the version of the paper presented here belong to the individual author(s) and/or other copyright owners. To the extent reasonable and practicable the material made available in WRAP has been checked for eligibility before being made available.

Copies of full items can be used for personal research or study, educational, or not-for-profit purposes without prior permission or charge. Provided that the authors, title and full bibliographic details are credited, a hyperlink and/or URL is given for the original metadata page and the content is not changed in any way.

**Publisher's statement:**

Please refer to the repository item page, publisher's statement section, for further information.

For more information, please contact the WRAP Team at: [wrap@warwick.ac.uk](mailto:wrap@warwick.ac.uk).

# Biguanide Iridium(III) Complexes with Potent Antimicrobial Activity

Feng Chen,<sup>†</sup> John Moat,<sup>‡</sup> Daniel McFeely,<sup>‡</sup> Guy Clarkson,<sup>†</sup> Ian J. Hands-Portman,<sup>‡</sup> Jessica P. Furner-Pardoe,<sup>‡</sup> Freya Harrison,<sup>‡\*</sup> Christopher G. Dowson<sup>‡\*</sup> and Peter J. Sadler<sup>†\*</sup>

<sup>†</sup> Department of Chemistry, University of Warwick, Gibbet Hill Road, Coventry CV4 7AL, UK.

<sup>‡</sup> School of Life Sciences, University of Warwick, Gibbet Hill Road, Coventry CV4 7AL, UK.

**ABSTRACT:** We have synthesized novel organo-iridium(III) antimicrobial complexes containing a chelated biguanide, including the antidiabetic drug metformin. These 16- and 18-electron complexes were characterized by NMR, ESI-MS, elemental analysis, and X-ray crystallography. Several of these complexes exhibit potent activity against Gram-negative bacteria and Gram-positive bacteria (including methicillin-resistant *Staphylococcus aureus* (MRSA), and high antifungal potency towards *C. albicans* and *C. neoformans*, with minimum inhibitory concentrations (MICs) in the nanomolar range. Importantly, the complexes exhibit low cytotoxicity towards mammalian cells, indicating high selectivity. They are highly stable in broth medium, with a low tendency to generate resistance mutations. On co-administration, they can restore the activity of vancomycin against vancomycin-resistant *Enterococci* (VRE). Also the complexes can disrupt and eradicate bacteria in mature biofilms. Investigations of reactions with biomolecules suggest that these organometallic complexes deliver active biguanides into microorganisms, whereas the biguanides themselves are inactive when administered alone.

## INTRODUCTION

Infectious diseases caused by drug resistant bacteria are currently the second main cause of death worldwide and the third leading cause of death in developed countries.<sup>1</sup> Fungal infections

are also a human health threat,<sup>2</sup> their clinical treatment presents profound challenges.<sup>3</sup> Gram-positive and Gram-negative bacteria have cell envelopes which guard against changes in osmotic pressure, chemical or enzymatic lysis and mechanical damage, and can survive under extreme conditions.<sup>4</sup> The cell wall of Gram-positive bacteria comprises a thick layer of peptidoglycan and the additional outer membrane of Gram-negative bacteria is populated with lipopolysaccharides, both of which features can protect bacteria from antibiotics.<sup>5,6</sup>

Drug resistance was originally found in hospitals where most antibiotics are used, e.g. sulfonamide-resistant *Streptococcus pyogenes* emerged in the 1930s and *Staphylococcus aureus* showed resistance to penicillin shortly after it was introduced in the 1940s.<sup>7</sup> Multidrug resistant bacteria, including the notorious *Enterococcus faecium*, *Staphylococcus aureus*, *Klebsiella pneumoniae*, *Acetivobacter baumannii*, *Pseudomonas aeruginosa*, and *Enterobacteriaceae* species, abbreviated as ‘ESKAPE’, are now a major threat to human health and cause of bacterial infectious diseases with high mortality.<sup>8-10</sup> Therefore, novel, effective, and safe antibiotics are urgently needed.<sup>11</sup>

Organometallic half-sandwich complexes provide a highly versatile platform for drug design.<sup>12</sup> The antiproliferative and antimicrobial activities of organometallic complexes can be fine-tuned by choice of the  $\pi$ -bonded arene or cyclopentadienyl ligand, the metal itself and its oxidation state, and by the other monodentate or chelating ligands.<sup>13</sup> We focus here on the third-row transition metal ion Ir<sup>III</sup>, which with its low-spin 5d<sup>6</sup> outer shell electronic configuration can be relatively inert and therefore likely to reach drug target sites with at least some of its initial ligands still bound.<sup>14</sup> So far, there are relatively few reports on the antimicrobial properties of organometallic iridium complexes.<sup>14-16</sup> Here we have introduced biguanide ligands into organo-iridium cyclopentadienyl complexes.

Biguanides are an important class of compounds that have wide pharmaceutical applications. One of the best known biguanide derivatives is the drug metformin (Metf), which has been used to treat type II diabetes for over 60 years. Other derivatives like phenformin, buformin, 1-phenylbiguanide and chlorophenylbiguanide are reported to exhibit antimicrobial and antiviral activity (**Chart 1**).<sup>17-20</sup> Jiang *et al.* have reported the synergistic effect of gold nanoparticles and metformin, generating broad-spectrum antibacterial and bactericidal activity against superbugs, with low cytotoxicity. Such nanoparticles decorated with biguanide ligands can penetrate cell membranes readily and have significant anti-biofilm activity.<sup>9</sup> Clardy *et al.* have synthesized norspermidine-mimicking guanide and biguanide compounds with activity in disrupting biofilms generated by *B. subtilis* and pathogenic *S. aureus*.<sup>21</sup> Over the last two decades, a library of biguanide chelated transition metal complexes has been studied, including  $[\text{Mn}^{\text{IV}}(\text{biguanide})_3]^{4+}$ ,  $[\text{Au}^{\text{III}}(\text{biguanide})]^+$ ,  $[\text{Cu}(\text{biguanide})_2]^{2+}$ ,  $[\text{Zn}(\text{biguanide})\text{Cl}_2]$ ,  $[\text{Pt}(\text{biguanide})\text{Cl}_2]$  and  $[\text{M}(\text{biguanide})]^{2+}$  (M: Mn, Co, Cu and Zn).<sup>22-26</sup> Some of those complexes show promising antimicrobial activity, but their mode of action (MoA) has yet to be elucidated.

Here we have synthesized and characterized a series of novel  $\text{Ir}^{\text{III}}$  complexes **1-14** containing either  $\text{Cp}^*$ ,  $\text{Cp}^{\text{Xph}}$  or  $\text{Cp}^{\text{Xbiph}}$ , a chelated metformin or an *N*-substituted biguanide, together with a monodentate halido ligand (**Chart 2**). Complexes and metal-free biguanides were screened against a broad range of microbes, including fungi, Gram-negative and Gram-positive bacteria. The synergistic effect of complexes **4**, **7** and **10** on co-administration with vancomycin against vancomycin-resistant *Enterococci* (VRE), was studied, as well as the anti-biofilm activity of complexes **4-9** in an *S. aureus* model. The bio-compatibility of selected complexes was studied towards human cells, as well as the stability of the complexes in culture medium, and the mutation rate of *S. aureus* treated with complexes **4**, **5** and **7**. We also investigated cell permeability and morphology changes in *S. aureus* induced by complex **7**, by confocal

microscopy and TEM, to gain insight into the mechanism of action. The interaction of complexes **4**, **7** and **10** with DNA nucleobase models 9-ethylguanine and guanosine-5'-monophosphate, and a variety of amino acids was investigated by  $^1\text{H}$  NMR and LC-MS to probe potential target sites.

## Results

### Synthesis and Characterization

Organometallic  $\text{Ir}^{\text{III}}$  complexes **1-14** were synthesised following a reported general procedure,<sup>27</sup> involving reaction of the appropriate chlorido-bridged  $\text{Ir}^{\text{III}}$  dimer and biguanide ligands in anhydrous methanol, to which triethylamine was added, followed by heating at 45 °C under nitrogen for 18 h. The dark red solids obtained after removal of solvent were purified by recrystallization (in MeOH and diethyl ether, 2:9 (v/v)) or on a silica chromatographic column using MeOH and DCM, 1:9(v/v) as eluents. Complexes **8** and **9** were synthesized by adding a 100-fold excess of NaBr or NaI, respectively.

Crystals of complexes **1**  $[(\text{Cp}^*)\text{Ir}(\text{Metf})\text{Cl}]\text{Cl}$  and **4**  $[(\text{Cp}^{\text{Xbiph}})\text{Ir}(\text{PhBig})]\text{Cl}$  suitable for X-ray structure determination were obtained by slow diffusion of diethyl ether into a saturated methanol solution of the complex at ambient temperature. The crystallographic data and selected bond lengths and angles are given in **Tables 1, S1-3**, and the crystal structures are shown in **Figure 1**. Complex **1** adopts a *pseudo*-octahedral structure with  $\text{Ir}^{\text{III}}$  bound to a  $\eta^5$ - $\text{Cp}^*$  ring, a chelated neutral metformin and chloride as ligands to form an 18e 1+ cation with 'piano-stool' geometry and chloride as the counter anion. In contrast, iridium in complex **4** is also a 1+ cation but bound only to a  $\eta^5$ - $\text{Cp}^{\text{Xbiph}}$  ring and deprotonated *N,N*-bound phenylbiguanide, giving a 16e species, with chloride as counter anion.

The asymmetric unit of complex **4** contains two crystallographically independent but chemically identical complexes, two chloride counter ions and a small amount of electron density modelled as a partially occupied methanol (40% occupancy). The Ir-N bond lengths of complex **1** are slightly longer than in complex **4**, **Table 1**. The C3-N3 and C5-N5 bond lengths of complex **1** are shorter than C3-N4 and C5-N4, and can be denoted as double bonds (**Table 1** and **Chart 2A**). While in complex **4**, the C110-N111 bond lengths are shorter than the respective C108-N108, and thus can be defined as double bonds (**Table 1** and **Chart 2B**). The N-Ir-N angle of complex **1** ( $83.21(12)^\circ$ ) is smaller than that of complex **4** ( $85.35(11)^\circ$ ). The structures of complexes **1** and **4** suggest that these novel Ir<sup>III</sup> complexes can be fine-tuned by the chelated ligands to result in 16 e or 18 e species.

### Relative Hydrophobicity

The relative hydrophobicities of complexes **1-14** were determined by RP-HPLC using a reverse-phase C<sub>18</sub> column. To ensure solubility of the Ir<sup>III</sup> complexes, MeOH/H<sub>2</sub>O, 1:9 v/v was used with NaCl (50 mM) present to suppress the hydrolysis. The HPLC eluents were also prepared with 50 mM NaCl (**Figure S1** in the Supporting Information). The resulting retention times are shown in **Table S4** in the Supporting Information. Complex **1** shows the shortest retention time (least hydrophobic) at 13.0 min. It is evident that complexes with more phenyl groups on the  $\eta^5$ -Cp<sup>X</sup> (complexes **2-3**), have higher retention times, indicating higher hydrophobicity. Complexes **4-9** with more hydrophobic functional phenyls on the chelating biguanide ligands have retention times range within 20.9-25.3 min, and the introduction of sulfonyl groups with aromatic substituents on the chelated biguanide ligands significantly enhances the hydrophobicity with retention time various of 32-37 min with the exception of complex **10** (toluene sulfonyl, 21.44 min) which was much less hydrophobic.

### Antimicrobial Activity

The minimum inhibitory concentrations (MICs) of complexes **1-14** were determined against Gram-negative bacterial strains: *Escherichia coli*, *Klebsiella pneumoniae*, *Pseudomonas aeruginosa*, *Acinetobacter baumannii*, and Gram-positive bacteria strains: *Bacillus subtilis*, *Streptococcus pyogenes*, *Enterococcus faecalis*, *Staphylococcus epidermidis* and *Staphylococcus aureus* (including methicillin-sensitive and -resistant (MRSA) strain types). Antifungal activity against *Candida albicans* and *Cryptococcus neoformans* was also studied. First, the antimicrobial activity of selected biguanide chelating ligands **L1-6** and **L10** against *E. coli*, *K. pneumoniae*, *P. aeruginosa*, *A. baumannii* and MRSA, and fungi was determined. None of these ligands exhibited activity, with MICs > 32 µg/mL.

The more hydrophilic Ir<sup>III</sup> complexes **1** and **2** are inactive against the majority of the pathogens studied, with MICs over 32 µg/mL (**Figure 2**), but the activity increased with increase in hydrophobicity (longer HPLC retention times), which is obvious seen from complex **3**, with MICs in the range 2- >32 µg/mL, probably due to the increased uptake of the complexes within the membranes of the bacteria.<sup>28</sup> This trend is also apparent from the antibacterial activity of complexes **1-4** against MRSA (**Figure S2** in the Supporting Information).

Among the Gram-negative bacteria, complexes **4-7** exhibit the highest potency against *A. baumannii* (MICs, 4 µg/mL (5.4-5.8 µM), an important nosocomial non-motile aerobic bacterial pathogen<sup>29</sup>) and *E. coli* (MICs 4-8 µg/mL (5.4-11.2 µM)) (**Figure 2** and **Table S4** in the Supporting Information). These complexes had moderate potency (MICs 16-32 µg/mL (21.6-44 µM)) towards *K. pneumoniae*, a cause of various nosocomial infections, *e. g.* urinary tract, pneumonia, and intra-abdominal infections (**Figure 2**).<sup>30</sup> However, all biguanide complexes have little activity towards *P. aeruginosa* (MICs above 32 µg/mL), probably due to the poor membrane permeability (only *ca.* 8% that of *E. coli*) and very effective efflux system,

which makes *P. aeruginosa* intrinsically resistant to many antibiotics (**Table S4** in the Supporting Information).<sup>31</sup>

In order to study the effect of halido ligand on the antimicrobial activity, the Cl in complex **7** were substituted by Br and I to obtain complexes **8** and **9**, respectively. To increase the hydrophobicity and potentially enhance uptake of the complexes, a sulfonyl group with an aromatic substituent was introduced onto the terminal nitrogen of the biguanide ligand, to obtain complexes **10-14** (**Chart 2**). Interestingly, complexes bromido **8** and iodido **9** showed higher antibacterial activity against *K. pneumoniae* compared to chloride complex **7**, but were less potent towards *E. coli* and *A. baumannii* (**Figure 2**). By introducing the sulfonyl substituents, the potency of complexes **10-14** decreased dramatically, with MICs all above 32 µg/mL (**Figure 2**).

The antifungal activity of complexes **1-14** was screened towards *C. albicans*, a common fungus in humans which can cause superficial mycoses, invasive mucosal infections, and disseminated systemic disease,<sup>32, 33</sup> and *C. neoformans*, an opportunistic yeast that can cause meningitis.<sup>34</sup> Interestingly, complexes **4-9** exhibited excellent antifungal activity against these fungi (MICs = 0.25-1 µg/mL (0.34-1.45 µM), **Figure 2**), *ca.* 76-fold more active against *C. neoformans* than the reference compound Fluconazole (8 µg/mL (26.1 µM), **Table S4** in the Supporting Information). The exchange of monodentate halido ligands had little effect on the antifungal activity (MICs 1 µg/mL (*ca.* 1.2 µM) and 0.5 µg/mL (*ca.* 0.6 µM), respectively). However, the introduction of sulfonyl functional groups lowered the activity slightly (MICs of complexes **10-14** of 1-2 µg/mL (1.1-2.4 µM), **Figure 2** and **Table S4** in the Supporting Information).

For Gram-positive bacteria, the antibacterial activity of complexes **1-14** was investigated in comparison with clinical drug vancomycin, and the minimum bactericidal concentrations (MBCs) were also determined. Generally, complexes **4-14** show moderate to excellent



antibacterial activity against Gram-positive bacteria strains, with MICs and MBCs within the range 0.125-32  $\mu\text{g/mL}$  (0.17-38  $\mu\text{M}$ , **Table 2**). In particular, complexes **4-9** exhibit potent inhibitory and bactericidal activity towards *S. pyogenes* and *S. epidermidis*, giving MIC and MBC in the range of 0.125-1  $\mu\text{g/mL}$  (0.17-1.5  $\mu\text{M}$ , **Table 2**). *S. pyogenes* is a pathogenic strain that responsible for *ca.* 517000 deaths annually,<sup>35</sup> which can cause benign to invasive diseases, *e.g.* necrotizing fasciitis, rheumatic fever and rheumatic heart disease.<sup>36</sup> *S. epidermidis* is an opportunistic microorganism which exists in human skin and mucosa;<sup>37</sup> the nosocomial genotypes are the main cause of catheter-related bloodstream, joint and biomedical device-related infections.<sup>38-40</sup> Complexes **4-9** also display potent antibacterial activity against *S. aureus* and *B. subtilis*, with MICs and MBCs in the range of 0.25-4  $\mu\text{g/mL}$  (0.3-2.9  $\mu\text{M}$ , **Table 2**).

*E. faecalis* is amongst the intestinal flora, and causes about 90% of enterococcal infections by inhibiting alimentary canals of man, which can induce lethal diseases. *E. faecalis* can survive in nosocomial environments due to intrinsic resistance to several antibiotics.<sup>41</sup> Complexes **4-9** show potent antibacterial activity against *E. faecalis* (MICs, 0.5-1  $\mu\text{g/mL}$  (0.58-1.45  $\mu\text{M}$ ), **Table 2**), *ca.* 4 $\times$  more potent than vancomycin (2.8  $\mu\text{M}$ ); and the MBCs range from 4-32  $\mu\text{g/mL}$  (5.5-43  $\mu\text{M}$ ). Sulfonyl-substituted complexes **10-14** exhibited significant inhibitory activity against *S. aureus*, *B. subtilis*, *S. pyogenes* and *S. epidermidis*, with MICs all below 1  $\mu\text{g/mL}$  (0.3-1.2  $\mu\text{M}$ , **Table 2**). However, the bactericidal activity of complexes **10-14** decreased dramatically, with MBCs against *S. aureus*, *S. epidermidis* and *E. faecalis* are >32  $\mu\text{g/mL}$  (>38  $\mu\text{M}$ ).

We next investigated whether generation of reactive oxygen species (ROS) could be a key process in the activity of the complexes. The MICs of complexes **4-10** were assessed under strict anaerobic conditions (generated with Oxoid AnaeroGen 2.5L sachets in a plastic container) for bacteria that lack superoxide dismutase (SOD) and so cannot quench the high levels of superoxide,<sup>42</sup> *S. aureus* (ATCC 29213) and *S. pyogenes* (ATCC 151112). As can be

seen from **Table S5**, there were no significant changes in MICs of complexes **4-10** compared with aerobic conditions, which suggests that ROS generation is not a key process in their activity.

### **Cytotoxicity (CC<sub>50</sub>), Haemolytic Activity (HC<sub>50</sub>) and Cytopathic Effects**

To investigate the selectivity of the complexes for microorganisms versus mammalian cells, the concentrations giving 50% cytotoxicity towards human embryonic kidney cells (*HEK-293*) and 50% haemolytic activity towards human red blood cells (*RBC*) for complexes **4-14** were determined (**Table 2**). In general, complexes **4-9** exhibited low *in vitro* cytotoxicity against *HEK-293* and *RBC* cells (CC<sub>50</sub>: 17 - >32 µg/mL (19 - >47 µM) and HC<sub>50</sub>: 6 - 21 µg/mL (8 - 28 µM)). Interestingly, complexes **8** (Br complex) and **9** (I complex) showed higher cytotoxicity (CC<sub>50</sub>, 27.6 µM and 18.6 µM, respectively) towards *HEK-293* cells than that of complex **7** (Cl complex, CC<sub>50</sub> value over 44 µM), decreasing in the order: **7** > **8** > **9**; while complexes **8** and **9** gave similar HC<sub>50</sub> values (8.2 and 8.6 µM, respectively), are lower than that of **7** (20 µM). As expected, complexes **10-14** displayed lower cytotoxicity (CC<sub>50</sub>: >32 µg/mL (>35 µM) and HC<sub>50</sub>: 15 - >32 µg/mL (17 - >35 µM)), when compared to complexes **4-9** (**Table 2**).

We also determined the cytopathic effect of a representative set of complexes **4-7**, **11**, **12** and **14** on *HaCaT* human keratinocyte cells (an immortalized, non-tumorigenic cell line, **Table 2**).<sup>43-45</sup> A 4 h-exposure of keratinocyte cells to these selected antimicrobial agents induced morphological changes in keratinocytes cells at concentrations of 128 µg/mL (139-179 µM) for **5-7** and **11-12**, and of 64 µg/mL (94 µM) and 32 µg/mL (35 µM) for complexes **4** and **14**, respectively; indicating the low cytotoxicity.

The selectivity factors (SF) of complexes **4-14** for the cytotoxicity against *HEK-293* (CC<sub>50</sub>, µM) and *RBC* (HC<sub>50</sub>, µM in brackets) versus the bactericidal activity towards Gram-positive bacteria (MIC, µM), are given in **Table S6** in the Supporting Information. SF values are the

ratio of CC<sub>50</sub> or HC<sub>50</sub> values to MBC values. Complexes **4-9** have good to excellent SF values between *S. aureus*, *B. subtilis*, *S. pyogenes* and *S. epidermidis*, with SF values in the range of 4 to >256 for CC<sub>50</sub>/MBC and 2 to 118 for HC<sub>50</sub>/MBC. However, the selectivity factors between *E. faecalis* and human cells for complexes **4-14** are poor, since these complexes have little activity towards this highly resistant pathogen.

### **Long-term Antibacterial Investigation**

The stability of complexes **4-10** by using *S. aureus* as model bacterium was investigated by determining their MICs after various time intervals (1-21 days). The complexes were dissolved in Cation-adjusted Mueller Hinton Broth at the concentration of 128 µg/mL and stored at three different temperatures: -18 °C, 18 °C and 42 °C. Antibacterial testing was performed on days 1, 4, 8 and 21 (**Table S7** in the Supporting Information). Little change in MICs of complexes **4-7** was observed after 21 days at 42 °C (in the range of 2-4 µg/mL), indicative of high stability. However, MICs of complexes **8-10** increased gradually from day 8 to day 21 at 42 °C, with MICs rising from 1 µg/mL to 16, 8 and 32 µg/mL, respectively, indicative of some degradation of these complexes at this temperature (42 °C).

### **Resistance Evolution**

To investigate the rate of generation of bacterial resistance towards these novel Ir<sup>III</sup> biguanide complexes, we determined the mutation rate of standard strain *S. aureus* exposed to complexes **4**, **5** and **7** at concentrations of 0.25 MIC, for sustained passages. MICs were determined after every 4 passages. After a total of 24 passages, MIC values of complexes **4**, **5** and **7** against *S. aureus* remained unchanged, suggesting that Gram-positive bacteria do not rapidly evolve resistance to these Ir<sup>III</sup> biguanide complexes.

### **Kinetics of Growth Inhibition**

The kinetics of growth inhibition by complex **7** was studied in three different *S. aureus* cultures of densities  $10^5$ ,  $10^7$  and  $10^8$  CFU/mL (**Figure 3a-c**), and the effect of DMSO concentration (1%, 5% and 10% DMSO in medium, v/v) in the broth medium on the cell growth (at bacterial intensity of  $10^5$  CFU/mL, **Figure 3d**). It is evident that high DMSO concentrations can greatly inhibit the bacterial growth (slow growth in 10% DMSO/90% medium). Concentrations of complex **7** in three ranges in bacterial medium culture were studied: 0.125 MIC to 2 MIC (cell density of  $1 \times 10^5$  CFU/mL), 0.25 MIC to 4 MIC ( $1 \times 10^7$  CFU/mL) and 0.5 MIC to 8 MIC ( $1 \times 10^8$  CFU/mL). As can be seen in the **Figure 3**, bacterial growth was well inhibited at MIC concentration when the cell culture density was  $1 \times 10^5$  CFU/mL; at higher cell culture densities ( $1 \times 10^7$  and  $1 \times 10^8$  CFU/mL), the total bacterial growth inhibition concentration of complex **7** increased to 2 MIC, but the complex inhibited the growth of *S. aureus* for *ca.* 500 min at MIC concentration when cell culture density was  $1 \times 10^7$  CFU/mL. Complex **7** exhibits a density-dependent antibacterial activity against *S. aureus*, consistent with MIC values. The growth of *S. aureus* was effectively hindered at sub-MIC and MIC concentrations of complex **7** at different culture cell densities, which indicates that these Ir<sup>III</sup> complexes may be sequestered inside bacteria cell and exhibit a constant bactericidal activity towards Gram-positive bacteria such as *S. aureus*.

### Synergistic Effects on Antibiotic Resistance

The intrinsic and acquired resistance of pathogens towards antibiotics has become a major problem.<sup>46</sup> Some newer antibiotics have little effect on highly resistant microorganisms.<sup>47</sup> Co-administration of new antibiotics with existing clinical drugs (to which pathogens have developed resistance) may re-activate their antimicrobial activity. Here we have investigated the synergistic activity of organo-iridium complexes **4**, **7** and **10** and the clinical drugs cefoxitin and vancomycin towards two highly resistant nosocomial pathogens: vancomycin-resistant *Enterococci* (VRE), methicillin-resistant *Staphylococcus aureus* (MRSA).

The MICs for co-administration of complexes **4**, **7** and **10** and the clinical drugs cefoxitin and vancomycin towards MRSA and VRE, respectively, were determined (**Table 3**, in the Supporting Information). The Ir<sup>III</sup> complexes themselves exhibit high antibacterial activity against VRE and MRSA with MICs of 0.5-4 µg/mL; while cefoxitin against MRSA and vancomycin against VRE give MIC values of 32 µg/mL and 64 µg/mL, respectively. As can be seen from **Table 3**, no synergistic effect of cefoxitin against MRSA was observed when co-administered with complexes **4**, **7** and **10** (at sub-MIC concentrations). Notably, the combination of complexes **4**, **7** and **10** with vancomycin towards VRE showed very high synergy, significantly decreasing the MIC values from 64 µg/mL to 0.25, 4 and 2 µg/mL, respectively (**Table 3**).

In further experiments, we examined the reverse synergistic effect upon co-incubation of vancomycin (at the concentrations of 0.25, 4 and 2 µg/mL) with complexes **4**, **7** and **10**. However, no growth inhibitory towards VRE below 0.5× MIC complex concentrations was observed after 24 h, at 37 °C.

### Anti-biofilm Study

Biofilms are integrations of microorganism communities with extracellular polymeric substances which consist mainly of a variety of bio-polymers.<sup>48</sup> The slow growth rate or low metabolism of organisms in biofilms makes the bacteria difficult to eradicate, and thus bacteria in biofilm are more tolerable to antibiotics.<sup>48,49</sup> Biguanide derivatives, both polymers<sup>50</sup> and low weight molecules<sup>21</sup> are reported as biofilm disruptors. We studied the ability of complexes **4-9** (at 100, 50, 30, 20, 10, 5 and 2 µg/mL) to kill *S. aureus* in biofilm model of soft-tissue biofilm infection. The logarithms of the numbers of bacterial colonies are listed in **Table S8**. A two-factor analysis of variance was carried out to compare the effectiveness of complexes with negative controls. It is evident from **Figure 4**, that after treatment of mature biofilms with Ir<sup>III</sup>

biguanide complexes, at the concentrations of 100 and 50  $\mu\text{g/mL}$ , at least a 3 log difference from the negative control is observed, suggesting that at such complex concentrations, over 99.9% of *S. aureus* are killed. Anti-biofilm efficacy at complex concentrations of 30 and 20  $\mu\text{g/mL}$  decreased significantly, but there was still a reduction of 1.5 and 1 log, respectively, compared to negative control, which indicates that  $\text{Ir}^{\text{III}}$  biguanide complexes can eradicate over 90% biofilm cells at equipotent 10 $\times$  to 15 $\times$  MIC concentrations. A decrease of cell viability was still observable, but very limited at lower complex concentrations (10, 5 and 2  $\mu\text{g/mL}$ ). Overall, there was a significant effect of each concentration on the number of CFU and this differed between the complexes (all  $p$ -values  $<0.01$ , see ANOVA **Table S9** in the Supporting Information)

### Induced Permeability Changes in Bacterial Cell Walls

In order to gain insight into the mechanism of the potent bactericidal activity of these complexes against Gram-positive bacteria, we evaluated the permeability change of bacterial cells based on a fluorescence DEAD/LIVE assay by exposure of *S. aureus* to complex **7** at 4 $\times$  MBC and 8 $\times$  MBC concentrations, with *S. aureus* without adding any antibiotic as negative control. The viability of bacteria was checked before being stained. Propidium Iodide (PI) is an effective dye which can bind uniquely to DNA or RNA nucleobase. PI itself cannot cross the membranes of viable cells, while dead cells with broken cell membranes are readily recognized by PI for intracellular staining.<sup>51,52</sup> It is evident from the images in **Figure 5a-c**, that little PI fluorescence was observed in negative control. The percentage of PI stained cells is *ca.* 6% on treatment with **7** at equipotent 4 $\times$  MBC concentration. Interestingly, this significantly up to *ca.* 28% at 8 $\times$  MBC concentration of **7**. However, either at 4 $\times$  MBC or 8 $\times$  MBC concentration of complex **7**, no obvious diffused fluorescence clusters were found, which implies that the bacterial cell membranes are intact and no leakage of nucleobases occurs.

Next, we investigated the change in morphology of cell walls by transmission electron microscopy (TEM). It is apparent from **Figure 5d**, that complex **7** did not break cell walls at equipotent concentrations of 10× MBC and 50× MBC. This is consistent with the confocal microscopy observations, which indicates that these biguanide Ir complexes are less likely to target bacterial cell walls.

### **Interaction with Nucleobases and Amino-Acids**

To provide preliminary indications of possible target sites for these potent antimicrobial biguanide complexes, we investigated reactions of some active complexes with nucleobases and amino acids.

The interaction of complexes **4** and **7** (2 mM, DMSO- $d_6$ /D $_2$ O, 2:3 (v:v)) with DNA nucleobases model 9-ethylguanine (9-EtG, 2 mM, D $_2$ O) and guanosine 5'-monophosphate disodium hydrate (5'-GMP, 2 mM, D $_2$ O) was investigated by NMR spectroscopy. No binding of complexes **4** and **7** to either 9-EtG or 5'-GMP was observed after 24 h incubation at pH\* 7.3, 37 °C. This suggests that DNA appears not to be the target for those novel complexes.

Next, the interaction of complexes **4**, **7** and **10** with the amino-acids (1 mole equiv) tryptophan, leucine, N-acetyl-L-methionine, L-histidine and L-cysteine (L-Cys) was studied on NMR, ESI-MS and LC-MS at pH 7.2. Samples were prepared and stored at 37 °C for 24 h. No reaction with tryptophan, leucine, N-acetyl-L-methionine or L-histidine was observed after 24 h incubation by ESI-MS (or LC-MS) and  $^1\text{H}$  NMR (data not shown). However these complexes can react rapidly with L-Cys, as shown for complexes **4** and **7** in **Figures S3** and **S4**, respectively, in the Supporting Information. Within 10 min at 37 °C, peaks for L-Cys had disappeared. The reactions appeared to proceed via L-Cys coordination followed by decomposition of the complex. This was investigated further by LC-MS.

The reaction of complexes **4**, **7** and **10** (0.2 mM, MeOH/H<sub>2</sub>O) with L-Cys (0.2 mM, H<sub>2</sub>O) was monitored by LC-MS after 24 h incubation at 37 °C, pH 7.1 (**Figure S5**, RP-HPLC eluents are given in **Figure S6** in the Supporting Information). Interestingly, complexes **4**, **7** and **10** formed the dinuclear dimer  $[(\text{Cp}^{\text{Xbiph}})\text{Ir}(\text{L-Cys})]_2^{2+}$  (**P2** in **Figure S5** in the Supporting Information)  $1171.39\ m/z$  (calculated  $[\text{C}_{48}\text{H}_{53}\text{Ir}_2\text{N}_2\text{O}_4\text{S}_2\text{-H}]^+$   $1171.27\ m/z$ ), with concomitant liberation of free biguanide ligands **L2** (phenylbiguanide + H<sup>+</sup>), **L5** (1-(o)-tolylbiguanide + H<sup>+</sup>) and **L6** (**P1**, TolSul-Big-Tol + H<sup>+</sup>).

## Discussion

### Antimicrobial Activity

The prevalence of antibiotic resistance towards the traditional clinical drugs has stimulated the development of more novel and potent antibiotics, especially the metal-based antimicrobial agents over the last decade.<sup>5</sup> A broad spectrum of organometallic complexes (e.g. Pt,<sup>53</sup> Cu,<sup>53</sup> Rh<sup>54</sup> and Ru<sup>55-57</sup>) as antimicrobial agents have been synthesized and studied for their antimicrobial activity. Collins and Keene *et. al.* have reported a series of mononuclear  $[\text{Ru}(\text{phen})_2(\text{bb}_7)]^{2+}$  and  $[\text{Ru}(\text{phen})_2(\text{bb}_{16})]^{2+}$ , dinuclear  $[\{\text{Ru}(\text{phen})_2\}_2\{\text{m-bb}_n\}]^{4+}$  and oligonuclear Ru<sup>II</sup> complexes, where bb<sub>n</sub> is bis[4(4'-methyl-2,2'-bipyridyl)]-1,n-alkane (n = 7, 12 or 16, *etc.*).<sup>58-61</sup> Those Ru<sup>II</sup> complexes showed potent antibacterial activity against *S. aureus* and MRSA, with MICs in the range of 0.3-16 µg/mL and MBCs in the range of 1-32 µg/mL;<sup>59, 61</sup> however, the dinuclear Ir<sup>III</sup> analogues  $[\{\text{Ir}(\text{tpy})\text{Cl}\}_2\{\mu\text{-bb}_n\}]\text{Cl}_4$  (n = 7, 12 and 16) exhibited lower antibacterial activity, with MICs over 128 µg/mL, the enhancement of charges from +2 (for Ru) to +3 (for Ir) may have an inverse effect on the antibacterial activity for dinuclear complexes.<sup>59</sup> Falkinham *et. al.* have reported  $[(\text{Cp}^{\text{XR}})\text{Ir}(1,2\text{-diamine-R}^1)\text{Cl}]\text{Cl}$  complexes, containing various R and R<sup>1</sup> aliphatic substituents;<sup>62</sup> these gave broad spectrum of anti-staphylococcal potency towards *S. aureus* and MRSA, with MICs in the scale of 4 to >500



$\mu\text{g/mL}$ . The introduction of substitutions on the amino groups lead to a decrease of biological activity, perhaps indicating that hydrogen bonding by  $\text{NH}_2$  of the diamine core is important for retaining the antibacterial potency.<sup>62</sup> In the present work,  $\text{Ir}^{\text{III}}$ -biguanide complexes **4-9** showed higher antibacterial activity against *S. aureus* and MRSA, with MICs as low as  $1 \mu\text{g/mL}$ , more potent than the reported  $\text{Ir}^{\text{III}}$  complexes.<sup>59, 62</sup> Complexes **3-9** are bactericidal towards the investigated Gram-positive bacteria, with the exception of *E. faecalis*, since the ratios of MBC/MIC for complexes **4-9** are within 2 (bactericidal activity denotes as a ratio of MBC to MIC no more than 4).<sup>63, 64</sup> Potent bacteriocidal activity is sometimes important for specific conditions, e.g. endocarditis from staphylococci infections.<sup>65</sup> In contrast, the introduction of sulfonyl groups on the terminal N of biguanide ligand **L5** significantly decreased bacteriocidal activity, making complexes **10-14** bacteriostatic (MBC/MIC > 4; **Table S10** in the Supporting Information) towards the Gram-positive bacteria, with the exception of *S. pyogenes*.<sup>63</sup>

Complexes **4-9** have potent antimicrobial activity, but relatively low cytotoxicity towards mammalian cells and low haemolytic activity (SF up to 256), indicative of good selectivity. Interestingly, bromo complex **8** and iodo complex **9** show higher potency in cytotoxicity and haemolytic activity than chlorido complex **7**, probably because complexes **8** and **9** are more inert and more stabilized from aquation; the complexes may remain intact before approaching intracellular targets, and this is in agreement with previous observations.<sup>66,67</sup> However, complexes **8** and **9** have similar antimicrobial activity (MIC), which is indistinctively different from complex **7**, suggesting that these complexes may have a different mode of action in killing microorganisms and human mammalian cells.

### Potential Targets and Mode of Action

These organometallic biguanide complexes contain a  $\pi$ -bonded  $\text{Cp}^{\text{X}}$  ligand which occupies 3 coordination sites and a chelated biguanide, ligand exchange at the 6<sup>th</sup> coordination site is

facile. In fact some complexes exist as either 16e or 18e species (**Chart 2**). The binding of the 6<sup>th</sup> ligand is therefore quite weak; no binding to the DNA nucleobase guanine (as 9-EtG or 5'-GMP) was detected, nor to the amino acids histidine, tryptophan and leucine. However, the thiol amino acid L-Cys reacted readily and displaced the biguanide ligand (**Figures S3 and S4** in the Supporting Information).

L-Cysteine is an important biosynthetic material for thiol-containing proteins and enzymes in cells, and is the major thiol donor for many intracellular cofactors, e.g. GSH (in eukaryotes and Gram-negative bacteria), Mycothiol (in Mycobacteria) and Bacillithiol (in many Gram-positive bacteria, i.e. *S. aureus* and *B. subtilis*).<sup>68, 69</sup> Bacteria, like cancer cells, are constantly under high oxidative stress. To cope with such stress, bacteria use these low-molecular weight thiols to detoxify xenobiotics.<sup>42</sup> Organometallic Ir<sup>III</sup> complexes have been reported to generate high levels of reactive oxygen species (ROS) in human cancer cells to induce the apoptosis;<sup>13</sup> however, the antibacterial activity (MIC) of complexes **4-10** against *S. aureus* and *S. pyogenes* under aerobic conditions is close to that under anaerobic conditions, suggesting that ROS generation is not critical for their antimicrobial activity.

From the DEAD/LIVE fluorescence staining and TEM study, the cell envelope remains intact after exposure to high complex concentrations (MBC to 8 MBC, **Figure 5**), indicating that these novel Ir<sup>III</sup> biguanide complexes are unlikely to target cell walls. The formation a [(Cp<sup>Xbiph</sup>)Ir(L-Cys)]<sub>2</sub><sup>2+</sup> dimer may play a key role in the mechanism of action together with the release of the free biguanide, inhibiting the biosynthesis of proteins and important cofactors. Agents which disrupt the cell wall or membrane, or interfere with essential enzymes, are often bactericidal, whereas agents which only inhibit protein synthesis tend to be bacteriostatic.<sup>70, 71</sup>

In the present study, the biguanide ligands alone are inactive towards all the microorganisms screened. Perhaps with their high basicity and overall positive charge, low hydrophobicity

limits biguanide uptake by bacteria. Biguanide derivatives including polyhexamethylene biguanide (PHMB) or chlorhexidine dihydrochloride, have been widely used as microbicides.<sup>72</sup> with biomembrane disruption being proposed as the prevailing mode of action. The guanidino groups of biguanides are highly basic ( $pK_a$  ca. 10.5-12.5) and cationic at pH 7, facilitating interactions with phospholipids via electrostatic forces. Adsorption of biguanides on the cell envelope perturbs lipids packing, leading to leakage of essential cellular molecules.<sup>73</sup> However, Good *et. al.* recently reported a DNA targeting mechanism for the biguanide PHMB, arresting cell division and inducing the condensation of bacterial chromosomal DNA.<sup>74</sup> Biguanide derivatives have strong metal-binding sites, and can bind to endogenous metal ions, and might inhibit enzymes.<sup>75</sup> For example biguanides such as phenformin inhibit pyruvate kinase.<sup>76</sup>

The Ir<sup>III</sup> biguanide complexes can act as delivery systems for transport of biguanides into bacteria. The complexes can react rapidly with thiol-containing biomolecules, e.g. L-cysteine, to form a  $[(Cp^{Xbiph})Ir(L-Cys)]_2^{2+}$  dimer, with the liberation of free biguanide ligands in the bacteria. The released biguanide ligands can bind to endogenous metal ions and might inhibit the important cell enzymes, e.g. pyruvate kinase, which play a key role in glycolysis regulation and are highly dependent on metal ions;<sup>77</sup> therefore bacteriocidal. However, the introduction of electron-withdrawing sulfonyl groups on the biguanide ligands lowers the  $pK_a$  (from >12 for ligand **L5** to  $4.7 \pm 0.1$  for **L6** (**Figure S7** in the Supporting Information)). Notably the sulfonyl complexes **10-14** are bacteriostatic in contrast to the bacteriocidal activity of the other complexes **4-9**, which is perhaps related to the activity of the released biguanide ligand and difference in charge (+1 versus 0 at pH 7).

## Conclusions

We have synthesized novel organo-iridium(III) antimicrobial complexes **1-14** containing a derivative of widely-used biguanides as a chelated ligand  $[(\eta^5-Cp^X)Ir(Big)Z]Z$  (where  $Cp^X =$

Cp\*, Cp<sup>Xph</sup> (phenyltetramethylcyclopentadienyl) or Cp<sup>Xbiph</sup> (biphenyltetramethylcyclopentadienyl), Big = a biguanide or sulfonyl-substituted biguanide ligand, Z = Cl, Br and I). The complexes were characterized by NMR, ESI-MS, elemental analysis, and X-ray crystallography.

Several of these complexes have potent activity against Gram-negative bacteria and Gram-positive bacteria, including MRSA with MICs as low as 0.125 µg/mL (0.17 µM, *ca.* 4× more potent than vancomycin). Notably, complexes **4-7** also exhibit high antifungal potency towards *C. albicans* and *C. neoformans*, with MIC values as low as 0.25 µg/mL (0.34 µM). Importantly, the complexes exhibit low cytotoxicity towards mammalian cells, indicating high selectivity. They are highly stable in broth medium, with a low tendency to generate resistance mutations.

Complexes **4**, **7** and **10** exhibit synergy with vancomycin against vancomycin-resistant *Enterococci* (VRE) when co-administered (up to *ca.* 256× enhancement of MIC). Also these complexes can disrupt and eradicate bacteria in mature biofilms. The high reactivity of these complexes towards L-cysteine, in contrast to other amino acids or nucleobases, with displacement of the biguanide ligand, suggests that their mechanism of action may involve intracellular biguanide release. In contrast the biguanides themselves are inactive when administered alone.

## Experimental Section

### Materials

Trihydrated iridium<sup>III</sup> trichloride was purchased from Precious Metals Online (PMO Pty Ltd.) and used as received. Biguanide ligands (metformin, 1-phenylbiguanide hydrochloride, 1-(4-Fluorophenyl) biguanide hydrochloride, 1-(o-Tolyl)biguanide and phenformin) were purchased from Sigma-Aldrich and used without further procession. All the sulfonyl chloride compounds used in this research were obtained from Sigma-Aldrich. High concentration rat tail collagen was obtained from Scientific Laboratory Supplies. Collagenase was obtained from VWR. Fetal bovine serum was purchased from Fisher Scientific, and peptone water and anaerobic atmosphere generation bag (Oxoid AnaeroGen 2.5L Sachets) were from Thermo Scientific. The NMR spectroscopy solvent, e.g. MeOD-d<sub>4</sub> and DMSO-d<sub>6</sub>, were purchased from Cambridge Isotope Laboratories Inc, and D<sub>2</sub>O and CDCl<sub>3</sub> were purchased from Sigma-Aldrich. The bacteria strains, *B. subtilis* DSM 10, *S. pyogenes* ATCC 151112, *E. faecalis* ATCC 29212, *S. aureus* ATCC 29213 and *S. epidermidis* ATCC 12228 were purchased from American Type Culture Collection (ATCC). The human keratinocyte cells were provided by Dr. Meera Unnikrishnan (University of Warwick). The remaining of the antimicrobial and cytotoxicity screens were carried out by CO-ADD from University of Queensland, Australia.

The purity of the synthesized materials has been determined to be  $\geq 95\%$  by elemental analysis, <sup>1</sup>H and <sup>13</sup>C NMR, high resolution MS, and RP-HPLC.

### Synthesis of Complexes 1-14

[(Cp\*)Ir(Metf)Cl]Cl (**1**). [(Cp\*)IrCl<sub>2</sub>]<sub>2</sub> (55.86 mg, 0.07 mmol) and metformin hydrochloride (25 mg, 0.15 mmol) were placed in a round-bottom flask to which anhydrous methanol (50 mL) and triethylamine (21  $\mu$ L, 0.15 mmol) were added. The solution was heated under refluxed

in a nitrogen atmosphere (50 °C) overnight. After which the solvent was removed on a rotary evaporator to give a red solid. The crude product was purified by recrystallization from mixed solvent of MeOH and diethyl ether (4:6, v:v), to obtain orange solid. Yield = 49 mg (66%). <sup>1</sup>H NMR (400 MHz, MeOD-d<sub>4</sub>): δ<sub>H</sub> 1.68 (s, 15H), 3.07 (s, 6H); <sup>13</sup>C NMR (125.73 MHz, D<sub>2</sub>O): δ<sub>C</sub> 8.2, 38.2, 88.5; HRMS (ESI): Calcd for [C<sub>14</sub>H<sub>26</sub>N<sub>5</sub>(Ir-HCl<sub>2</sub>)]<sup>+</sup> 456.1739 *m/z*, found: 456.1734 *m/z*. Anal. Calcd for C<sub>14</sub>H<sub>26</sub> Cl<sub>2</sub>N<sub>5</sub>Ir(H<sub>2</sub>O)<sub>0.5</sub>: C, 31.34; H, 5.07; N, 13.05. Found: C, 31.29; H, 4.78; N, 12.87.

**[(Cp<sup>Xph</sup>)Ir(Metf)Cl]Cl (2).** Complex **2** was synthesized following the method similar to complex **1**, where [(Cp<sup>Xph</sup>)IrCl<sub>2</sub>]<sub>2</sub> (150 mg, 0.163 mmol), metformin hydrochloride (55 mg, 0.33 mmol) and triethylamine (92 μL, 0.66 mmol) were used. The crude product was purified by recrystallization from mixed solvent of MeOH and diethyl ether (4:6, v:v), to obtain yellow solid. Yield = 104 mg (54%). <sup>1</sup>H NMR (300 MHz, D<sub>2</sub>O): δ<sub>H</sub> 1.71 (s, 6H), 1.84 (s, 6H), 3.09 (s, 6H), 7.52 (s, 5H); <sup>13</sup>C NMR (125.73 MHz, D<sub>2</sub>O): δ<sub>C</sub> 8.3, 8.9, 38.2, 88.3, 92.0, 129.0, 129.1, 129.5, 130.2; HRMS (ESI): Calcd for [C<sub>19</sub>H<sub>27</sub>N<sub>5</sub>(Ir-HCl<sub>2</sub>)]<sup>+</sup> 518.1896 *m/z*, found: 518.1893 *m/z*. Anal. Calcd for C<sub>19</sub>H<sub>28</sub>Cl<sub>2</sub>IrN<sub>5</sub>: C, 38.71; H, 4.79; N, 11.88. Found: C, 38.60; H, 4.79; N, 11.50.

**[(Cp<sup>Xbiph</sup>)Ir(Metf)Cl]Cl (3).** Complex **3** was synthesized following the method similar to complex **1**, where [(Cp<sup>Xbiph</sup>)IrCl<sub>2</sub>]<sub>2</sub> (100 mg, 0.093 mmol), metformin hydrochloride (32 mg, 0.188 mmol) and triethylamine (53 μL, 0.376 mmol) were used. The crude product was purified on a chromatography column (DCM/MeOH (10:1, v:v), to obtain red solid. Yield = 72 mg (58%). <sup>1</sup>H NMR (300 MHz, MeOD-d<sub>4</sub>): δ<sub>H</sub> 1.94 (s, 6H), 2.05 (s, 6H), 3.16 (s, 6H), 4.60 (s, 2H), 7.38-7.43 (m, 1H), 7.49 (t, *J* = 8.1 Hz, 2H), 7.67 (q, *J* = 7.7 Hz, 15.0 Hz, 4H), 7.78 (d, *J* = 7.4 Hz, 2H); <sup>13</sup>C NMR (125.73 MHz, D<sub>2</sub>O): δ<sub>C</sub> 8.8, 9.3, 37.2, 90.0, 91.1, 126.8, 127.3, 128.2, 129.2, 130.9, 139.4, 141.2; HRMS (ESI): Calcd for [C<sub>25</sub>H<sub>31</sub>N<sub>5</sub>(Ir-Cl)]<sup>+</sup> 594.2209 *m/z*, found: 594.2204

$m/z$ . Anal. Calcd for  $C_{25}H_{31}ClIrN_5(H_2O)_{0.5}$ : C, 47.05; H, 5.05; N, 10.97. Found: C, 46.88; H, 4.86; N, 10.63.

**[(Cp<sup>Xbiph</sup>)Ir(PhBig)Cl] (4).** Complex **4** was synthesized following the method similar to complex **1**, where [(Cp<sup>Xbiph</sup>)IrCl<sub>2</sub>]<sub>2</sub> (100 mg, 0.093 mmol), 1-phenylbiguanide hydrochloride (41 mg, 0.188 mmol) and triethylamine (53  $\mu$ L, 0.376 mmol) were used. The crude product was purified on a chromatography column (DCM/MeOH (10:1, v:v), to obtain dark red solid. Yield = 57 mg (45%). <sup>1</sup>H NMR (400 MHz, DMSO-d<sub>6</sub>):  $\delta_H$  1.90 (s, 6H), 1.98 (s, 6H), 6.44 (s, 2H), 6.94 (t,  $J$  = 7.1 Hz, 1H), 7.24 (t,  $J$  = 7.8 Hz, 2H), 7.41 (t,  $J$  = 7.0 Hz, 1H), 7.50 (t,  $J$  = 7.6 Hz, 2H), 7.56 (d,  $J$  = 8.1 Hz, 2H), 7.63 (d,  $J$  = 8.2 Hz, 2H), 7.72 (d,  $J$  = 7.6 Hz, 2H), 7.77 (d,  $J$  = 8.1 Hz, 2H), 9.18 (s, 2H), 9.24 (s, 1H); <sup>13</sup>C NMR (125.73 MHz, CDCl<sub>3</sub>):  $\delta_C$  127.0, 127.9, 128.0, 129.0, 129.6, 130.5; HRMS (ESI): Calcd for [C<sub>29</sub>H<sub>31</sub>N<sub>5</sub>(Ir-Cl)]<sup>+</sup> 642.2209  $m/z$ , found: 642.2209  $m/z$ . Anal. Calcd for  $C_{29}H_{31}ClIrN_5(H_2O)_{0.5}$ : C, 50.75; H, 4.70; N, 10.21. Found: C, 50.78; H, 4.54; N, 10.10.

**[(Cp<sup>Xbiph</sup>)Ir(4-F-PhBig)Cl] (5).** Complex **5** was synthesized following the method similar to complex **1**, where [(Cp<sup>Xbiph</sup>)IrCl<sub>2</sub>]<sub>2</sub> (200 mg, 0.187 mmol), 1-(4-fluorophenyl)biguanide hydrochloride (93 mg, 0.4 mmol) and triethylamine (112  $\mu$ L, 0.8 mmol) were added. The crude product was purified on a chromatography column (DCM/MeOH (10:1, v:v), to obtain dark red solid. Yield = 118 mg (43%). <sup>1</sup>H NMR (400 MHz, MeOD-d<sub>4</sub>):  $\delta_H$  1.96 (s, 6H), 2.06 (s, 6H), 7.05 (t,  $J$  = 8.6 Hz, 2H), 7.41 (t,  $J$  = 7.2 Hz, 1H), 7.47-7.51 (m, 4H), 7.64 (d,  $J$  = 8.2 Hz, 2H), 7.96 (d,  $J$  = 7.4 Hz, 2H), 7.77 (d,  $J$  = 8.2 Hz, 2H); <sup>13</sup>C NMR (125.73 MHz, CDCl<sub>3</sub>):  $\delta_C$  127.0, 127.9, 128.0, 129.1, 130.6; <sup>19</sup>F NMR (376.4 MHz, D<sub>2</sub>O):  $\delta_F$  -121.8; HRMS (ESI): Calcd for [C<sub>29</sub>H<sub>30</sub>FN<sub>5</sub>(Ir-Cl)]<sup>+</sup> 660.2114  $m/z$ , found: 660.2105  $m/z$ . Anal. Calcd for  $C_{29}H_{30}ClIrN_5(H_2O)_{0.9}$ : C, 48.96; H, 4.51; N, 9.84. Found: C, 48.97; H, 4.19; N, 9.77.

**[(Cp<sup>Xbiph</sup>)Ir(PhenethylBig)Cl]Cl (6).** Complex **6** was synthesized following the method similar to complex **1**, where [(Cp<sup>Xbiph</sup>)IrCl<sub>2</sub>]<sub>2</sub> (200 mg, 0.187 mmol), phenformin hydrochloride (92 mg, 0.38 mmol) and triethylamine (110  $\mu$ L, 0.76 mmol) were added. The crude product was purified on a chromatography column (DCM/MeOH (10:1, v:v), to give dark red solid. Yield = 183 mg (66%). <sup>1</sup>H NMR (300 MHz, MeOD-d<sub>4</sub>):  $\delta_{\text{H}}$  1.93 (s, 6H), 2.02 (s, 6H), 3.49-3.58 (m, 4H), 4.60 (s, 3H), 7.20-7.29 (m, 5H), 7.42 (d,  $J$  = 6.5 Hz, 1H), 7.47-7.52 (m, 2H), 7.61 (d,  $J$  = 7.7 Hz, 2H), 7.68 (d,  $J$  = 7.6 Hz, 2H), 7.75 (d,  $J$  = 7.5 Hz, 2H); <sup>13</sup>C NMR (125.73 MHz, MeOD-d<sub>4</sub>):  $\delta_{\text{C}}$  42.4, 126.6, 127.3, 127.6, 128.1, 128.5, 128.7, 130.9; HRMS (ESI): Calcd for [C<sub>31</sub>H<sub>34</sub>N<sub>5</sub>(Ir-HCl<sub>2</sub>)]<sup>+</sup> 670.2522  $m/z$ , found: 670.2519  $m/z$ . Anal. Calcd for C<sub>31</sub>H<sub>36</sub>Cl<sub>2</sub>IrN<sub>5</sub>: C, 50.20; H, 4.89; N, 9.44. Found: C, 50.74; H, 4.88; N, 9.38.

**[(Cp<sup>Xbiph</sup>)Ir(TolBig)Cl]Cl (7).** Complex **7** was synthesized following the method similar to complex **1**, where [(Cp<sup>Xbiph</sup>)IrCl<sub>2</sub>]<sub>2</sub> (200 mg, 0.187 mmol), 1-(o-tolyl)biguanide (73 mg, 0.38 mmol) and triethylamine (110  $\mu$ L, 0.76 mmol) were added. The crude product was purified on a chromatography column (DCM/MeOH (10:1, v:v), to get a dark red solid. Yield = 125 mg (46%). <sup>1</sup>H NMR (300 MHz, MeOD-d<sub>4</sub>):  $\delta_{\text{H}}$  1.92 (s, 6H), 2.04 (s, 6H), 2.26 (s, 3H), 7.11-7.16 (m, 1H), 7.21 (d,  $J$  = 7.7 MHz, 1H), 7.28 (d,  $J$  = 7.7 Hz, 1H), 7.38-7.44 (m, 2H), 7.48-7.53 (m, 2H), 7.57 (d,  $J$  = 7.5 Hz, 2H), 7.71 (t,  $J$  = 8.6 Hz, 4H); <sup>13</sup>C NMR (125.73 MHz, CDCl<sub>3</sub>):  $\delta_{\text{C}}$  126.8, 127.0, 127.3, 127.4, 127.9, 128.0, 129.1, 130.2, 131.7; HRMS (ESI): Calcd for [C<sub>30</sub>H<sub>33</sub>N<sub>5</sub>(Ir-HCl<sub>2</sub>)]<sup>+</sup> 656.2365  $m/z$ , found: 656.2362  $m/z$ . Anal. Calcd for C<sub>30</sub>H<sub>34</sub>Cl<sub>2</sub>IrN<sub>5</sub>: C, 49.51; H, 4.71; N, 9.62. Found: C, 49.49; H, 4.46; N, 9.69.

**[(Cp<sup>Xbiph</sup>)Ir(TolBig)Br]Br (8).** [(Cp<sup>Xbiph</sup>)IrCl<sub>2</sub>]<sub>2</sub> (100 mg, 0.093 mmol) in methanol (30 mL) and sodium bromide (1.92 g, 18.7 mmol) in deionised water (10 mL) were mixed in a round bottom flask. The solution was heated to 70 °C for 1 h. Then, a solution of 1-(o-tolyl)biguanide (36.6 mg, 0.191 mmol) and triethylamine (54  $\mu$ L, 0.383 mmol) were added, the reaction was



heated at 70 °C under nitrogen atmosphere for 12 h. After which the solvent was removed on a rotary evaporator to get a dark red solid. The solid was re-dissolved in chloroform and washed with brine (3 × 50 mL), and dried over MgSO<sub>4</sub>. The crude product was further purified on a chromatography column (DCM/MeOH (20:1, v:v), to give a reddish-brown solid. Yield = 100 mg (65%). <sup>1</sup>H NMR (400 MHz, MeOD-d<sub>4</sub>): δ<sub>H</sub> 1.69 (s, 6H), 1.82 (s, 6H), 2.14 (s, 3H), 7.31 (t, *J* = 7.6 Hz, 1H), 7.10 (t, *J* = 6.8 Hz, 1H), 7.17 (d, *J* = 7.3 Hz, 2H), 7.30 (t, *J* = 7.4 Hz, 1H), 7.39 (t, *J* = 7.2 Hz, 4H), 7.56 (t, *J* = 7.4 Hz, 4H); <sup>13</sup>C NMR (125.73 MHz, CDCl<sub>3</sub>): δ<sub>C</sub> 16.6, 65.5, 126.6, 127.3, 127.5, 128.7, 130.5, 140.0; HRMS (ESI): *Calcd* for [C<sub>30</sub>H<sub>33</sub>N<sub>5</sub>(Ir-HBr<sub>2</sub>)]<sup>+</sup> 656.2365 *m/z*, found: 656.2376 *m/z*. Anal. *Calcd* for C<sub>30</sub>H<sub>34</sub>Br<sub>2</sub>IrN<sub>5</sub>(Et<sub>2</sub>O)<sub>0.6</sub>: C, 45.19; H, 4.68; N, 8.13. Found: C, 45.24; H, 4.32; N, 8.33.

**[(Cp<sup>Xbiph</sup>)Ir(TolBig)I]I (9).** [(Cp<sup>Xbiph</sup>)IrCl<sub>2</sub>]<sub>2</sub> (100 mg, 0.093 mmol) in methanol (30 mL) and potassium iodide (3.1 g, 18.7 mmol) in deionised water (10 mL) were mixed in a round bottom flask. The solution was heated to 70 °C for 1 h. Then, a solution of 1-(o-tolyl)biguanide (36.6 mg, 0.191 mmol) and triethylamine (54 μL, 0.383 mmol) were added, the reaction was heated at 70 °C under nitrogen atmosphere for 12 h and a scarlet precipitate was observed. After which the solvent was removed on a rotary evaporator to get a dark red solid. The solid was re-dissolved in chloroform and washed with brine (3 × 50 mL), and dried over MgSO<sub>4</sub>. The crude product was further purified on a chromatography column (DCM/MeOH (20:1, v:v), to give an orange solid. Yield = 102 mg (59%). <sup>1</sup>H NMR (400 MHz, MeOD-d<sub>4</sub>): δ<sub>H</sub> 1.76 (s, 6H), 1.90 (s, 6H), 2.23 (s, 3H), 7.11-7.18 (m, 3H), 7.26 (d, *J* = 7.4 Hz, 1H), 7.41 (d, *J* = 8.0 Hz, 3H), 7.50 (t, *J* = 7.4 Hz, 2H), 7.59 (d, *J* = 8.2 Hz, 2H), 7.66 (d, *J* = 7.2 Hz, 2H); <sup>13</sup>C NMR (125.73 MHz, CDCl<sub>3</sub>): δ<sub>C</sub> 8.3, 9.0, 16.7, 126.6, 127.2, 127.5, 128.7, 130.4, 131.3, 140.0, 141.2; HRMS (ESI): *Calcd* for [C<sub>30</sub>H<sub>34</sub>IN<sub>5</sub>(Ir-I)]<sup>+</sup> 784.1488 *m/z*, found: 784.1488 *m/z*. Anal. *Calcd* for C<sub>30</sub>H<sub>34</sub>I<sub>2</sub>IrN<sub>5</sub>: C, 39.57; H, 3.76; N, 7.69. Found: C, 39.96; H, 3.77; N, 7.60.

**[(Cp<sup>Xbiph</sup>)Ir(TolSul-Big-Tol)Cl] (10).** Complex **10** was synthesized following the method similar to complex **1**, where [(Cp<sup>Xbiph</sup>)IrCl<sub>2</sub>]<sub>2</sub> (130 mg, 0.121 mmol), 4-methyl-N-(N-(N-(o-tolyl)carbamimidoyl)carbamimidoyl)benzenesulfonamide (93 mg, 0.269 mmol) and triethylamine (110  $\mu$ L, 0.76 mmol) were added. The crude product was purified on a chromatography column (DCM/MeOH (25:1, v:v), to give a yellow solid. Yield = 139 mg (68%). <sup>1</sup>H NMR (400 MHz, MeOD-d<sub>4</sub>):  $\delta_{\text{H}}$  1.53 (s, 6H), 1.72 (s, 6H), 2.17 (s, 3H), 2.30 (s, 3H), 7.17-7.22 (m, 5H), 7.27 (d, *J* = 6.9 Hz, 1H), 7.36 (d, *J* = 8.2 Hz, 2H), 7.40 (d, *J* = 7.4 Hz, 1H), 7.49 (t, *J* = 7.4 Hz, 2H), 7.57 (d, *J* = 8.2 Hz, 2H), 7.65-7.67 (m, 4H); <sup>13</sup>C NMR (125.73 MHz, MeOD-d<sub>4</sub>):  $\delta_{\text{C}}$  8.7, 18.0, 21.4, 126.1, 127.0, 127.6, 127.6, 128.9, 129.2, 130.4, 131.5, 133.8, 140.3, 140.8, 141.3, 141.4, 151.7, 152.9; HRMS (ESI): Calcd for [C<sub>37</sub>H<sub>39</sub>N<sub>5</sub>O<sub>2</sub>S(Ir-Cl)]<sup>+</sup> 810.2454 *m/z*, found: 810.2449 *m/z*. Anal. Calcd for C<sub>37</sub>H<sub>39</sub>ClIrN<sub>5</sub>O<sub>2</sub>S(H<sub>2</sub>O)<sub>0.4</sub>: C, 52.12; H, 4.70; N, 8.21. Found: C: 52.16, H: 4.62, N: 8.07.

**[(Cp<sup>Xbiph</sup>)Ir(4-(BrCH<sub>2</sub>)-PhSul-Big-Tol)Cl] (11).** Complex **11** was synthesized following the method similar to complex **1**, where [(Cp<sup>Xbiph</sup>)IrCl<sub>2</sub>]<sub>2</sub> (200 mg, 0.187 mmol), 4-(bromomethyl)-N-(N-(N-(o-tolyl)carbamimidoyl)carbamimidoyl)benzenesulfonamide (173.6 mg, 0.410 mmol) and triethylamine (116  $\mu$ L, 0.83 mmol) were added. The crude product was purified on a chromatography column (DCM/MeOH (25:1, v:v), to give a yellow solid. Yield = 131 mg (38%). <sup>1</sup>H NMR (300 MHz, MeOD-d<sub>4</sub>):  $\delta_{\text{H}}$  1.56 (s, 6H), 1.75 (s, 6H), 2.18 (s, 3H), 2.32 (s, 1H), 4.60 (s, 1H), 7.19-7.22 (m, 3H), 7.27 (d, *J* = 8.8 Hz, 1H), 7.37-7.52 (m, 5H), 7.57-7.59 (m, 2H), 7.67 (d, *J* = 9.2 Hz, 3H), 7.79 (d, *J* = 10.4 Hz, 1H); <sup>13</sup>C NMR (125.73 MHz, MeOD-d<sub>4</sub>):  $\delta_{\text{C}}$  7.6, 8.4, 16.5, 44.4, 91.2, 126.2, 126.6, 127.2, 127.2, 127.3, 127.5, 128.6, 128.7, 128.9, 129.1, 130.4, 131.3, 140.1; HRMS (ESI): Calcd for [C<sub>37</sub>H<sub>38</sub>N<sub>5</sub>O<sub>2</sub>SBr(Ir-Cl)]<sup>+</sup> 888.1559 *m/z*, found: 888.1551 *m/z*. Anal. Calcd for C<sub>37</sub>H<sub>38</sub>ClBrIrN<sub>5</sub>O<sub>2</sub>S: C, 48.08; H, 4.14; N, 7.58. Found: C, 48.09; H, 4.14; N, 7.45.

**[(Cp<sup>Xbiph</sup>)Ir(4-F-PhSul-Big-Tol)Cl] (12).** Complex **12** was synthesized following the method similar to complex **1**, where [(Cp<sup>Xbiph</sup>)IrCl<sub>2</sub>]<sub>2</sub> (150 mg, 0.140 mmol), 4-fluoro-N-(N-(N-(o-tolyl)carbamimidoyl)carbamimidoyl)benzenesulfonamide (103 mg, 0.294 mmol) and triethylamine (82  $\mu$ L, 0.588 mmol) were used. The crude product was purified on a chromatography column (DCM/MeOH (25:1, v:v), to give a yellow solid. Yield = 84 mg (48%). <sup>1</sup>H NMR (400 MHz, MeOD-d<sub>4</sub>):  $\delta_{\text{H}}$  1.58 (s, 6H), 1.75 (s, 6H), 2.18 (s, 3H), 7.12-7.22 (m, 5H), 7.28 (d,  $J$  = 6.9 Hz, 1H), 7.38-7.41 (m, 3H), 7.49 (t,  $J$  = 7.4 Hz, 2H), 7.60 (d,  $J$  = 8.1 Hz, 2H), 7.67 (d,  $J$  = 7.4 Hz, 2H), 7.82 (t,  $J$  = 7.5 Hz, 2H); <sup>13</sup>C NMR (125.73 MHz, MeOD-d<sub>4</sub>):  $\delta_{\text{C}}$  7.4, 8.3, 16.4, 91.4, 115.2, 115.4, 126.6, 127.2, 127.2, 127.5, 127.8, 128.7, 130.4, 131.3, 140.0, 141.4; <sup>19</sup>F NMR (376.38 MHz, MeOD-d<sub>4</sub>):  $\delta_{\text{F}}$  -109.97; ESI-MS: Calcd for [C<sub>36</sub>H<sub>36</sub>N<sub>5</sub>O<sub>2</sub>SF(Ir-Cl)]<sup>+</sup> 814.2203 m/z, found: 814.2200 m/z. Anal. Calcd for C<sub>36</sub>H<sub>36</sub>ClFIrN<sub>5</sub>O<sub>2</sub>S: C 50.90, H: 4.27, N: 8.24; Found: C, 50.56; H, 4.26; N, 8.20.

**[(Cp<sup>Xbiph</sup>)Ir(4-NO<sub>2</sub>-PhSul-Big-Tol)Cl] (13).** Complex **13** was synthesized following the method similar to complex **1**, where [(Cp<sup>Xbiph</sup>)IrCl<sub>2</sub>]<sub>2</sub> (110 mg, 0.103 mmol), 4-nitro-N-(N-(N-(o-tolyl)carbamimidoyl)carbamimidoyl)benzenesulfonamide (86 mg, 0.228 mmol) and triethylamine (64  $\mu$ L, 0.455 mmol) were added. The crude product was purified on a chromatography column (DCM/MeOH (25:1, v:v), and yellow solid was obtained. Yield = 162 mg (66%). <sup>1</sup>H NMR (400 MHz, MeOD-d<sub>4</sub>):  $\delta_{\text{H}}$  1.58 (s, 6H), 1.75 (s, 6H), 2.18 (s, 3H), 7.18-7.21 (m, 3H), 7.27 (d,  $J$  = 6.9 Hz, 1H), 7.37-7.41 (m, 3H), 7.49 (t,  $J$  = 7.4 Hz, 2H), 7.58 (d,  $J$  = 8.0 Hz, 2H), 7.65 (d,  $J$  = 7.7 Hz, 2H), 8.02 (d,  $J$  = 8.6 Hz, 2H), 8.25 (d,  $J$  = 8.3 Hz, 2H); <sup>13</sup>C NMR (125.73 MHz, MeOD-d<sub>4</sub>):  $\delta_{\text{C}}$  7.5, 8.3, 16.4, 123.5, 126.6, 127.1, 127.2, 127.5, 128.7, 130.4, 131.2, 140.0; ESI-MS: Calcd for [C<sub>36</sub>H<sub>36</sub>N<sub>6</sub>O<sub>4</sub>S(Ir-Cl)]<sup>+</sup> 841.2148 m/z, found: 841.2143 m/z. Anal. Calcd for C<sub>36</sub>H<sub>36</sub>IrN<sub>6</sub>O<sub>4</sub>S: C, 49.33; H, 4.14; N, 9.59. Found: C, 49.14; H, 4.06; N, 9.49.

**[(Cp<sup>Xbiph</sup>)Ir(Dan-Big-Tol)Cl] (14).** Complex **14** was synthesized following the method similar to complex **1**, where [(Cp<sup>Xbiph</sup>)IrCl<sub>2</sub>]<sub>2</sub> (120 mg, 0.112 mmol), 5-(dimethylamino)-N-(N-(N-(o-tolyl)carbamimidoyl)carbamimidoyl)naphthalene-1-sulfonamide (100 mg, 0.236 mmol) and triethylamine (66  $\mu$ L, 0.472 mmol) were added. The crude product was purified on a chromatography column (DCM/MeOH (25:1, v:v), to give yellow solid. Yield = 91.2 mg (44%). <sup>1</sup>H NMR (400 MHz, MeOD-d<sub>4</sub>):  $\delta_{\text{H}}$  1.45 (s, 6H), 1.68 (s, 6H), 2.06 (s, 3H), 2.76 (s, 6H), 7.11 (s, 1H), 7.17-7.24 (m, 6H), 7.36-7.41 (m, 4H), 7.47-7.54 (m, 3H), 7.60 (d,  $J$  = 7.4 Hz, 2H), 8.06 (d,  $J$  = 6.8 Hz, 1H), 8.40 (d,  $J$  = 8.5 Hz, 1H), 8.56 (d,  $J$  = 8.6 Hz, 1H); <sup>13</sup>C NMR (125.73 MHz, MeOD-d<sub>4</sub>):  $\delta_{\text{C}}$  7.4, 8.2, 16.3, 44.3, 91.9, 114.7, 122.9, 126.6, 127.0, 127.1, 127.1, 127.2, 127.5, 128.7, 129.9, 130.3, 131.3, 140.0, 151.4; HRMS (ESI): Calcd for [C<sub>42</sub>H<sub>44</sub>N<sub>6</sub>O<sub>2</sub>S (Ir-Cl)]<sup>+</sup> 889.2876  $m/z$ , found: 889.2883  $m/z$ . Anal. Calcd for C<sub>42</sub>H<sub>44</sub>ClIrN<sub>6</sub>O<sub>2</sub>S: C, 54.56; H, 4.80; N, 9.09. Found: C, 54.23; H, 4.77; N, 8.75.

### NMR Spectroscopy

<sup>1</sup>H NMR spectra were acquired at 298 K on either a Bruker HD-400, or HD-500 spectrometer using 5 mm NMR tubes. Data were processed out using TopSpin 3.5pl7 version (Bruker U.K. Ltd.). <sup>1</sup>H NMR chemical shifts were internally referenced to TMS via 1, 4-dioxane in D<sub>2</sub>O ( $\delta$  = 3.75) or residual MeOD-d<sub>4</sub> ( $\delta$  = 3.31 ppm) or CDCl<sub>3</sub> ( $\delta$  = 7.26 ppm). 1D spectra were recorded using standard pulse sequences.

### High Resolution Mass Spectrometry and Elemental Analysis

Elemental analyses were performed by Warwick Analytical Service using an Exeter Analytical elemental analyzer (CE440). High Resolution Mass Spectrometry (HRMS) Data were obtained on Bruker Maxis Plus Q-TOF.

### X-ray Crystallography

Single crystals of complexes **1** and **4** were grown from methanol/diethyl ether. Suitable crystals were selected and mounted on a glass fibre and placed on an Xcalibur Gemini diffractometer with a Ruby CCD area detector. The crystal was kept at  $-123 \pm 2$  °C during data collection. The structures were solved with the ShelXT<sup>78</sup> structure solution program using Direct Methods, and refined with the ShelXL<sup>79</sup> refinement package using Least Squares minimisation. The crystal data have been deposited at the Cambridge Crystallographic Data Centre with numbers: CCDC 1846267 and 1846268 for complexes **1** and **4**, respectively.

### **Relative Hydrophobicity**

Since log P determinations on metal complexes are often complicated by hydrolysis of metal-halide bonds in traditional octanol-water systems, we have used RP-HPLC to compare relative hydrophobicities.<sup>80</sup> These measurements were performed utilizing the Agilent 1200 system with a VWD and 50  $\mu$ L loop. The column was an Agilent Zorbax 300SB C18, 150  $\times$  4.6 mm with a 5  $\mu$ m pore size. The mobile phase was H<sub>2</sub>O (50 mM NaCl)/H<sub>2</sub>O/CH<sub>3</sub>CN 1:1 (50 mM NaCl), with a flow of 1 mL min<sup>-1</sup>. The detection wavelength was set at 254 nm with the reference wavelength at 360 nm. All compounds were dissolved in 10% MeOH/90% H<sub>2</sub>O (v/v) in 50 mM NaCl to ensure that hydrolysis was prevented. Sample injections were the loop volume (50  $\mu$ L) with needle washes of H<sub>2</sub>O and MeOH between injections. Reported retention times (tR) and standard deviations (SD) are from duplicates of triplicate measurements. The gradient used is shown in **Figure S1**.

### **Liquid Chromatography–Mass Spectrometry (LC-MS)**

LC-MS was performed on a HP 1200 Series HPLC System (Agilent) coupled to a Bruker HCT-Ultra ETD II PTR PTM mass spectrometer. The column used was an Agilent ZORBAX Eclipse Plus C-18 (4.6  $\times$  250 mm, 5  $\mu$ m pore size). The mobile phases were A: water (HPLC grade, with 0.1% TFA), and B: acetonitrile (HPLC grade, with 0.1% TFA). Samples were prepared

in double deionized water (DDW), with 50  $\mu$ L injection for each running. The mass spectrometer was operated in electrospray positive mode with scan range 50-2000  $m/z$ . The gradient used is shown in **Figure S6**.

### **Antibacterial Assays**

The minimum inhibitory concentrations (MICs) against a variety of Gram-positive bacteria studied by us was determined by the broth microdilution method as described in the CLSI guidelines.<sup>81</sup> The bacteria strains studied were cultured in Cation-adjusted Mueller Hinton Broth (CAMHB) and diluted to give the concentration of  $5 \times 10^5$  CFU/mL. The complexes in broth were serially diluted in the sterile 96-well plate to give the volume of 100  $\mu$ L. The media solutions with bacteria were then dispensed to each well cell to make the final volume of 200  $\mu$ L and the final concentration of Ir<sup>III</sup> complexes ranged in 0.125-256  $\mu$ g/mL, all the plates were covered and incubated at 37 °C for 18 h without shaking. Inhibition of bacterial growth was determined measuring absorbance at 600 nm (OD<sub>600</sub>), using a Tecan SPARK 10M plate reader. The negative control (media only) and positive control (bacteria without inhibitors) on the same plate were used as references to determine the growth inhibition of bacteria. Samples with inhibition value above 90% were classified as active agents. The minimum bactericidal concentrations (MBCs) were determined by treating the agar plate with 5  $\mu$ L sample solutions from each well with no visible growth observed. The agar plates were placed in a 37 °C oven for 18 h without shaking (*S. pyogenes* were incubated under a 5% CO<sub>2</sub> atmosphere). The ones had no colony formed with minimum concentrations will be MBCs.

### **Resistance Evolution**

The standard bacterial strain *S. aureus* (ATCC 29213) was cultured in HB medium (1 mL) in the presence of 0.25  $\mu$ g/mL (1/4 of MICs) of complexes **4**, **5** and **7**, and overnight incubation at 37 °C was considered as the first passage. At the second day, 40  $\mu$ L of bacteria medium was

added to the prepared complex stockings (1 mL), and such a treatment was repeated for 24 times (count as 24 passages). The antibacterial activity of complexes **4** and **7** against the treated *S. aureus* was determined by culturing the microbe on agar plate containing complexes **4**, **5** and **7** (at MIC concentrations) every 4 days.

### **Kinetics of Growth Inhibition**

Bacteria strain *S. aureus* (Type: ATCC 29213) was cultured in CAMHB overnight at 37 °C. Three bacteria suspensions of  $1 \times 10^5$ ,  $1 \times 10^7$  and  $1 \times 10^8$  CFU/mL were prepared by culture dilution. Complex in broth was diluted to give the concentration  $0.125 \times \text{MIC}$  to  $8 \times \text{MIC}$ . The negative control (media only) and positive control (culture bacteria with DMSO (1% - 10%)) were used as comparison. The measurement of absorbance at OD<sub>600</sub> was determined on a Tecan SPARK 10M plate reader with shaking for 18 h at 37 °C, the absorbance was detected every 5 min for the first one hour and every 30 min for the rest 17 h. No growth was observed for negative control.

### **Biofilm Cultivation and Antibiotic Treatment**

Biofilms were prepared according to a reported literature procedure, with modifications.<sup>82</sup> Generally, bacteria strain *S. aureus* (ATCC 29213) was cultured in synthetic wound fluid (SWF, consisting of 50% fetal bovine serum and 50% autoclaved peptone water, v/v) at 37 °C on an orbital shaker. In a sterile falcon tube, polymerized rat tail collagen matrix was prepared and kept on an ice bath. Typically, 10 mL collagen matrix, 2 mL collagen stock solution (10 mg/mL), was mixed with 6 mL SWF, 1 mL 0.1%, v/v acetic acid and 1 mL 0.1 M NaOH. After mixing, 400 µL of the collagen matrix was added to separate wells of 24-well polystyrene microtiter plates without introducing bubbles and placed at 37 °C for 1 h to allow collagen to polymerise. Then 100 µL of diluted bacterial culture (OD<sub>600</sub> of ca. 0.1 in SWF) was added to

each collagen matrix. The plate was incubated at 37 °C without shaking for 24 h to allow growth of biofilms in the collagen matrix.

The tested complexes (200 µL of complexes **4-9**, in DMSO/H<sub>2</sub>O, 5/95(v/v)) were added to the 24-h-old biofilms in triplicate and placed at 37 °C for a further 24 h. Then 600 µL of collagenase (0.5 mg/mL in PBS) was added to each wound, and incubated at 37 °C for 1 h to dissolve the collagen matrix. Serial dilutions of each wound were made in PBS using a sterile 96-well plate, and 10 µL of each dilution dropped onto an LB agar plate in triplicate for colony counting and calculation of viable cell numbers in the treated and untreated biofilms.

We used R to fit an ANOVA on log-transformed data to determine the effect of complex identity and concentration (and their interaction) on numbers of viable bacteria (**Table S10** in the Supporting Information).<sup>82</sup> We then used the *lsmeans* package to perform a one-sided test of whether each concentration of each complex led to a reduction in numbers of viable bacteria,<sup>84</sup> compared with the mean number of bacteria recovered from 9 replica untreated cultures (which was 3.03e+9). A Tukey correction for multiple comparisons was used.

### **Live/Dead Cell Assessment by PI Staining**

$1 \times 10^8$  CFU/mL of *S. aureus* cells were seeded in 50-mL Falcon tubes and exposed to two concentrations of complex **7** (equipotent MIC and 2 MIC) for 2 h without shake. *S. aureus* cells without any antibiotics were used as negative comparison. After indicated incubation time, cell suspensions were collected by centrifugation at 8000 rpm for 10 min and washed with PBS (0.01 M) 3 times. The cell pellets were then re-suspended in water in 2 mL eppendorf tubes and treated with 3 µM PI for 30 min in the dark at room temperature. Excessive PI was removed by washing cells with PBS 3 times, and 20 µL of samples were placed on a glass slide with a glass coverslip. The fluorescence of each glass slide was detected on a confocal microscope (LSM 880, AxioObserver) at excitation and emission wavelengths of 514/642 nm.



## Transmission Electron Microscopy

$5 \times 10^8$  CFU/mL of *S. aureus* cells were cultured in 50-mL Falcon tubes and exposed to two concentrations of complex **7** (10 MBC and 50 MBC) at 37 °C for 2 h without shake. After incubation, the cell suspensions were harvested by centrifugation at 8000 rpm for 3 min and washed with PBS (0.01 M) 2 times at 4 °C. The cells were fixed by 2.5% glutaraldehyde in PBS at 4 °C for 1 h, washed with PBS and water, and centrifuged. Then the bacterial pellet was re-suspended in 10% ethanol, and dehydrated with 20%-100% ethanol with 20 min of each. Cells were left in 100% fresh ethanol for over 24 h. Then the cell pellets were left in propylene oxide for 2 h, propylene/LV resin (1:1, v/v) for 5 h and 100% LV resin overnight. After which, cells were polymerised at 65 °C for 24 h and cut on Ultracut E Microtome to 100 nm and stained with 4% uranyl acetate. Finally, TEM monitoring was carried out on Jeol 2011 LaB6 filament with Gatan Ultrascan 1000 camera.

## ASSOCIATED CONTENT

### Supporting Information

The Supporting Information is available free of charge on the ACS Publications website at DOI: xxxx

Crystallographic data (**Table S1-3**), antimicrobial activity and RP-HPLC retention times (**Table S4**), antibacterial activity under aerobic and anaerobic conditions (**Table S5**), selectivity factors and stability testing (**Tables S6 and S7**), antibacterial activity of complexes and clinical drugs (**Table S8**), effect of biofilm disruption data (**Tables S9 and S10**), MBC/MIC ratios (**Table S11**); and relative hydrophobicity measurements (**Figure S1**), correlation of retention times with MICs (**Figure S2**),  $^1\text{H}$  NMR spectra of L-Cys reactions (**Figures S3 and S4**) and biguanide pH titrations, (**Figure S7**), LC-MS monitoring of L-Cys reactions and eluents used (**Figures S5 and S6**) (PDF)

Molecular formula strings of complexes **1-14** (CSV)

## **AUTHOR INFORMATION**

### **Corresponding Authors**

\*E-mail: p.j.sadler@warwick.ac.uk

E-mail: C.G.Dowson@warwick.ac.uk

E-mail: F.Harrison@warwick.ac.uk

### **Author Contributions**

P. J. S. designed and coordinated the overall experimental programme, with the help of C. G. D. and F. H. (with the help of CO-ADD). F. C. synthesized and characterized the complexes and studied their chemical reactions, C. G. D., F. C., J. M. and D. McF. designed and carried out the microbiological growth and inhibition studies, F. C., F. H. and J. P. F.-P. carried out the biofilm studies, G. J. C. the X-ray crystallography, and I. J. H.-P. the imaging studies. F. C., P. J. S. and F. H. wrote the manuscript and all authors contributed to the final version.

### **Notes**

The authors declare no competing financial interest.

### **Acknowledgements.**

Antimicrobial screening was partially performed by CO-ADD (The Community for Antimicrobial Drug Discovery), funded by the Wellcome Trust (UK) and The University of Queensland (Australia). We thank the EPSRC (grants EP/F034210/1, EP/P030572/1, and EP/M027503/1), and China Scholarship Council (CSC; scholarship for F.C.) for support. We also thank Phillip Aston, Dr Lijiang Song and Dr. Ivan Prokes for their excellent assistance

with mass spectrometry and NMR spectroscopy, and Professor Garry Graham (UNSW) for stimulating discussions on metformin pharmacology.

### Abbreviations Used

ATCC, American Type Culture Collection; ANOVA, analysis of variance; Biph, biphenyl; 4-(BrCH<sub>2</sub>)-PhSul-Big-Tol, 4-(Bromomethyl)-N-(N-(N-(o-tolyl)carbamimidoyl)carbamimidoyl) benzenesulphonamide; CAMHB, cation-adjusted mueller hinton broth; CCDC, Cambridge crystallographic data centre; Cef, Cefoxitin; CFU, colony forming unit; CO-ADD, Community for Open Antimicrobial Drug Discovery; CC<sub>50</sub>, concentrations giving 50% cytotoxicity; Cp\*, pentamethylcyclopentadienyl; Dan-Big-Tol, 5-(Dimethylamino)-N-(N-(N-(o-tolyl)carbamimidoyl)carbamimidoyl) naphthalene-1-sulfonamide; DSM, Deutsche Sammlung von Mikroorganismen; 9-EtG, 9-ethylguanine; 4-F-PhSul-Big-Tol, 4-fluoro-N-(N-(N-(o-tolyl)carbamimidoyl)carbamimidoyl) benzenesulfonamide; 4-F-PhBig, 1-(4-fluorophenyl)biguanide; 5'-GMP, guanosine 5'-monophosphate; HaCaT, keratinocyte cell line; HC<sub>50</sub>, 50% haemolytic activity; L-Cys, L-cysteine; Metf, metformin; TolSul-Big-Tol, 4-methyl-N-(N-(N-(o-tolyl)carbamimidoyl)carbamimidoyl) benzenesulfonamide; MBC, minimum bactericidal concentration; MoA, mode of action; 4-NO<sub>2</sub>-PhSul-Big-Tol, 4-nitro-N-(N-(N-(o-tolyl)carbamimidoyl)carbamimidoyl) benzenesulfonamide; PhBig, 1-phenylbiguanide; PhEtBig, phenformin; TolBig, 1-(o-tolyl)biguanide; pK<sub>a</sub>, acid dissociation constant; PHMB, polyhexamethylene biguanide; PI, propidium iodide; SF, selectivity factor; SWF, synthetic wound fluid; tR, retention times; Van, vancomycin; VRE, vancomycin resistant *Enterococci*

## References

- (1) Nathan, C. Antibiotics at the crossroads. *Nature* **2004**, *431*, 899-902.
- (2) Fisher, M. C.; Hawkins, N. J.; Sanglard, D.; Gurr, S. J. Worldwide emergence of resistance to antifungal drugs challenges human health and food security. *Science* **2018**, *360*, 739–742.
- (3) Geddes-McAlister, J.; Shapiro, R. S. New pathogens, new tricks: emerging, drug-resistant fungal pathogens and future prospects for antifungal therapeutics. *Ann. N.Y. Acad. Sci.* [Online early access]. DOI: 10.1111/nyas.13739. Published Online: May 15, 2018. <https://nyaspubs.onlinelibrary.wiley.com/doi/abs/10.1111/nyas.13739> (accessed May 15, 2018).
- (4) Li, F.; Collins, J. G.; Keene, F. R. Ruthenium complexes as antimicrobial agents. *Chem. Soc. Rev.* **2015**, *44*, 2529–2542.
- (5) Feng, Z. V.; Gunsolus, I. L.; Qiu, T. A.; Hurley, K. R.; Nyberg, L. H.; Frew, H.; Johnson, K. P.; Vartanian, A. M.; Jacob, L. M.; Lohse, S. E.; Torelli, M. D.; Hamers, R. J.; Murphy, C. J.; Haynes, C. L. Impacts of gold nanoparticle charge and ligand type on surface binding and toxicity to Gram-negative and Gram-positive bacteria. *Chem. Sci.* **2015**, *6*, 5186–5196.
- (6) Papo, N.; Shai, Y. A Molecular mechanism for lipopolysaccharide protection of Gram-negative bacteria from antimicrobial peptides. *J. Biol. Chem.* **2005**, *280*, 10378–10387.
- (7) Levy, S. B.; Marshall, B. Antibacterial resistance worldwide: causes, challenges and responses. *Nat. Med.* **2004**, *10*, 122-129.
- (8) Ng, N. S.; Leverett, P.; Hibbs, D. E.; Yang, Q.; Bulanadi, J. C.; Wu, M.; Aldrich-Wright, J. R. The antimicrobial properties of some copper(II) and platinum(II) 1,10-phenanthroline complexes. *Dalton Trans.* **2013**, *42*, 3196–3209.
- (9) Zhao, Y.; Chen, Z.; Chen, Y.; Xu, J.; Li, J.; Jiang, X. Synergy of non-antibiotic drugs and pyrimidinethiol on gold nanoparticles against superbugs. *J. Am. Chem. Soc.* **2013**, *135*, 12940–12943.

- (10) Bouley, R.; Ding, D.; Peng, Z.; Bastian, M.; Lastochkin, E.; Song, W.; Suckow, M. A.; Schroeder, V. A.; Wolter, W. R.; Mobashery, S.; Chang, M. Structure–activity relationship for the 4(3H)-quinazolinone antibacterials. *J. Med. Chem.* **2016**, *59*, 5011–5021.
- (11) Nussbaum, F. v.; Brands, M.; Hinzen, B.; Weigand, S.; Häbich, D. Antibacterial natural products in medicinal chemistry-exodus or revival?. *Angew. Chem. Int. Ed.* **2006**, *45*, 5072–5129.
- (12) Noffke, A. L.; Habtemariam, A.; Pizarro, A. M.; Sadler, P. J. Designing organometallic compounds for catalysis and therapy. *Chem. Commun.* **2012**, *48*, 5219–5246.
- (13) Tripathy, S. K.; Taviti, A. C.; Dehury, N.; Sahoo, A.; Pal, S.; Beuria, T. K.; Patra, S. Synthesis, characterisation and antibacterial activity of  $[(p\text{-cym})\text{RuX}(\text{L})]^{+/2+}$  (X = Cl, H<sub>2</sub>O; L = bpmo, bpms). *Dalton Trans.* **2015**, *44*, 5114–5124.
- (14) Liu, Z.; Sadler, P. J. Organoiridium complexes: anticancer agents and catalysts. *Acc. Chem. Res.* **2014**, *47*, 1174–1185.
- (15) Simpson, P. V.; Schmidt, C.; Ott, I.; Bruhn, H.; Schatzschneider, U. Synthesis, cellular uptake and biological activity against pathogenic microorganisms and cancer cells of rhodium and iridium N-heterocyclic carbene complexes bearing charged substituents. *Eur. J. Inorg. Chem.* **2013**, *2013*, 5547–5554.
- (16) Jain, N.; Alam, P.; Laskar, I. R.; Panwar, J. ‘Aggregation induced phosphorescence’ active iridium(III) complexes for integrated sensing and inhibition of bacterial growth in aqueous solution. *RSC Adv.* **2015**, *5*, 61983–61988.
- (17) Thomas, L.; Russell, A. D.; Maillard, J. Y. Antimicrobial activity of chlorhexidine diacetate and benzalkonium chloride against *Pseudomonas aeruginosa* and its response to biocide residues. *J. Appl. Microbiol.* **2005**, *98*, 533–543.
- (18) Denys, A.; Machlanski, T.; Bialek, J.; Mrozicki, S. Relation between chemical structure and antiviral activity of some biguanide derivatives. *Praeventivmedizin* **1977**, *164*, 85–89.

- (19) Bharatam, P. V.; Patel, D. S.; Iqbal, P. Pharmacophoric features of biguanide derivatives: an electronic and structural analysis. *J. Med. Chem.* **2005**, *48*, 7615-7622.
- (20) Samart, N.; Beuning, C. N.; Haller, K. J.; Rithner, C. D.; Crans, D. C. Interaction of a biguanide compound with membrane model interface systems: probing the properties of antimalarial and antidiabetic compounds. *Langmuir* **2014**, *30*, 8697–8706.
- (21) Böttcher, T.; Kolodkin-Gal, I.; Kolter, R.; Losick, R.; Clardy, J. Synthesis and activity of biomimetic biofilm disruptors. *J. Am. Chem. Soc.* **2013**, *135*, 2927–2930.
- (22) Das, G.; Bharadwaj, P. K.; Ghosh, D.; Chaudhuri, B.; Banerjee, R. Synthesis and structure of the  $[\text{Mn}^{\text{IV}}(\text{biguanide})_3]^{4+}$  ion: the simplest source for water-stable manganese(IV). *Chem. Commun.* **2001**, *0*, 323–324.
- (23) Zhang, J.; Sun, R. W.; Che, C. M. A dual cytotoxic and anti-angiogenic water-soluble gold (III) complex induces endoplasmic reticulum damage in HeLa cells. *Chem. Commun.* **2012**, *48*, 3388–3390.
- (24) Quan, X.; Uddin, R.; Heiskanen, A.; Parmvi, M.; Nilson, K.; Donolato, M.; Hansen, M. F.; Renac, G.; Boisen, A. The copper binding properties of metformin – QCM-D, XPS and nanobead agglomeration. *Chem. Commun.* **2015**, *51*, 17313–17316.
- (25) Olar, R.; Badea, M.; Cristurean, E.; Lazar, V.; Cernat, R.; Balotescu, C. Thermal behavior, spectroscopic and biological characterization of Co(II), Zn(II), Pd(II) and Pt(II) complexes with N, N-dimethylbiguanide. *J. Therm. Anal. Cal.* **2005**, *80*, 451–455.
- (26) Olar, R.; Badea, M.; Marinescu, D.; Chifiriuc, M.; Bleotu, C.; Grecu, M. N.; Iorgulescu, E.; Lazar, V. N, N-dimethylbiguanide complexes displaying low cytotoxicity as potential large spectrum antimicrobial agents. *Eur. J. Med. Chem.* **2010**, *45*, 3027-3034.
- (27) Soldevila-Barreda, J. J.; Bruijninx, P. C. A.; Habtemariam, A.; Clarkson, G. J.; Deeth, R. J.; Sadler, P. J. Improved catalytic activity of ruthenium–arene complexes in the reduction of  $\text{NAD}^+$ . *Organometallics* **2012**, *31*, 5958-5967.

- (28) Millett, A. J.; Habtemariam, A.; Romero-Canelón, I.; Clarkson, G. J.; Sadler, P. J. Contrasting anticancer activity of half-sandwich iridium(III) complexes bearing functionally diverse 2-phenylpyridine ligands. *Organometallics* **2015**, *34*, 2683–2694.
- (29) Yun, S.; Choi, C.; Kwon, S.; Park, G. W.; Cho, K.; Kwon, K.; Kim, J. Y.; Yoo, J. S.; Lee, J. C.; Choi, J.; Kim, S. Quantitative proteomic analysis of cell wall and plasma membrane fractions from multidrug-resistant *Acinetobacter baumannii*. *J. Proteome Res.* **2011**, *10*, 459–469.
- (30) Worthington, R. J.; Bunders, C. A.; Reed, C. S.; Melander, C. Small molecule suppression of carbapenem resistance in NDM-1 producing *Klebsiella pneumoniae*. *ACS Med. Chem. Lett.* **2012**, *3*, 357–361.
- (31) Hancock, R. E. W.; Brinkman, F. S. L. Function of *Pseudomonas* porins in uptake and efflux. *Annu. Rev. Microbiol.* **2002**, *56*, 17–38.
- (32) Xu, Y.; Wang, Y.; Yan, L.; Liang, R.; Dai, B.; Tang, R.; Gao, P.; Jiang, Y. Proteomic analysis reveals a synergistic mechanism of fluconazole and berberine against fluconazole-resistant *Candida albicans*: endogenous ROS augmentation. *J. Proteome Res.* **2009**, *8*, 5296–5304.
- (33) Yan, L.; Zhang, J.; Cao, Y.; Gao, P.; Jiang, Y. Proteomic analysis reveals a metabolism shift in a laboratory fluconazole-resistant *Candida albicans* strain. *J. Proteome Res.* **2007**, *6*, 2248–2256.
- (34) Zerpa, R.; Huicho, L.; Guillen, A. Modified India ink preparation for *Cryptococcus neoformans* in cerebrospinal fluid specimens. *J. Clin. Microbiol.* **1996**, *34*, 2290–2291.
- (35) Zaman, M.; Abdel-Aal, A. B. M.; Fujita, Y.; Ziora, Z. M.; Batzloff, M. R.; Good, M. F.; Toth, I. Structure–activity relationship for the development of a self-adjuvanting mucosally active lipopeptide vaccine against *Streptococcus pyogenes*. *J. Med. Chem.* **2012**, *55*, 8515–8523.

- (36) Ferretti, J. J.; Stevens, D. L.; Bryant, A. E. *Streptococcus pyogenes*: Basic Biology to Clinical Manifestations. Oklahoma City (OK): University of Oklahoma Health Sciences Center, **2016**.
- (37) Otto, M. *Staphylococcus epidermidis*—the “accidental” pathogen. *Nat. Rev. Microbiol.* **2009**, *7*, 555–567.
- (38) Widerström, M. Significance of *Staphylococcus epidermidis* in health care-associated infections, from contaminant to clinically relevant pathogen: this is a wake-up call!. *J. Clin. Microbiol.* **2016**, *54*, 1679–1681.
- (39) Pavlovsky, L.; Sturtevant, R. A.; Younger, J. G.; Solomon, M. J. Effects of temperature on the morphological, polymeric, and mechanical properties of *Staphylococcus epidermidis* bacterial biofilms. *Langmuir* **2015**, *31*, 2036–2042.
- (40) O’Gara, J. P.; Humphreys, H. *Staphylococcus epidermidis* biofilms: importance and implications. *J. Med. Microbiol.* **2001**, *50*, 582–587.
- (41) Jeong, K. W.; Lee, J. Y.; Kang, D.; Lee, J. U.; Shin, S. Y.; Kim, Y. Screening of flavonoids as candidate antibiotics against *Enterococcus faecalis*. *J. Nat. Prod.* **2009**, *72*, 719–724.
- (42) Dharmaraja, A. T. Role of reactive oxygen species (ROS) in therapeutics and drug resistance in cancer and bacteria. *J. Med. Chem.* **2017**, *60*, 3221–3240.
- (43) Boukamp, P.; Petrussevska, R. T.; Breitkreutz, D.; Hornung, J.; Markham, A.; Fusenig, N. E. Normal keratinization in a spontaneously immortalized aneuploid human keratinocyte cell line. *J. Cell Biol.* **1988**, *106*, 761–771.
- (44) Amigo, M.; Terencio, M. C.; Mitova, M.; Iodice, C.; Paya, M.; DeRosa, S. Potential antipsoriatic avarol derivatives as antioxidants and inhibitors of PGE(2) generation and proliferation in the *HaCaT* cell line. *J. Nat. Prod.* **2004**, *67*, 1459–1463.



- (45) Lau, W. M.; Ng, K. W.; White, A. W.; Heard, C. M. Therapeutic and cytotoxic effects of the novel antipsoriasis codrug, Naproxyl–Dithranol, on *HaCaT* cells. *Mol. Pharmaceutics* **2011**, *8*, 2398–2407.
- (46) Lainson, J. C.; Daly, S. M.; Triplett, K.; Johnston, S. A.; Hall, P. R.; Diehnelt, C. W. Synthetic antibacterial peptide exhibits synergy with oxacillin against *MRSA*. *ACS Med. Chem. Lett.* **2017**, *8*, 853–857.
- (47) Mohammad, H.; Younis, W.; Chen, L.; Peters, C. E.; Pogliano, J.; Pogliano, K.; Cooper, B.; Zhang, J.; Mayhoub, A.; Oldfield, E.; Cushman, M.; Seleem, M. N. Phenylthiazole antibacterial agents targeting cell wall synthesis exhibit potent activity *in vitro* and *in vivo* against vancomycin-resistant *Enterococci*. *J. Med. Chem.* **2017**, *60*, 2425–2438.
- (48) Abee, T.; Kovacs, A. T.; Kuipers, O. P.; van der Veen, S. Biofilm formation and dispersal in Gram-positive bacteria. *Curr. Opin. Biotechnol.* **2011**, *22*, 172–179.
- (49) Donlan, R. M.; Costerton, J. W. Biofilms: survival mechanisms of clinically relevant microorganisms. *Clin. Microbiol. Rev.* **2002**, *15*, 167–193.
- (50) Kamaruzzaman, N. F.; Chong, S. Q. Y.; Edmondson-Brown, K. M.; Ntow-Boahene, W.; Bardiau, M.; Good, L. Bactericidal and anti-biofilm effects of polyhexamethylene biguanide in models of intracellular and biofilm of *Staphylococcus aureus* isolated from bovine mastitis. *Front. Microbiol.* **2017**, *8*, 1518–1527.
- (51) Zhao, Y.; Tian, Y.; Cui, Y.; Liu, W.; Ma, W.; Jiang, X. Small molecule-capped gold nanoparticles as potent antibacterial agents that target Gram-negative bacteria. *J. Am. Chem. Soc.* **2010**, *132*, 12349–12356.
- (52) Hoque, J.; Akkapeddi, P.; Yadav, V.; Manjunath, G. B.; Uppu, D. S. S. M.; Konai, M. M.; Yarlagadda, V.; Sanyal, K.; Haldar, J. Broad spectrum antibacterial and antifungal polymeric paint materials: synthesis, structure–activity relationship, and membrane-active mode of action. *ACS Appl. Mater. Interfaces* **2015**, *7*, 1804–1815.

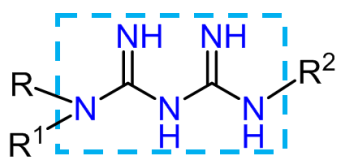
- (53) Yuan, Z.; Shen, X.; Huang, J. Syntheses, crystal structures and antimicrobial activities of Cu(II), Ru(II), and Pt(II) compounds with an anthracene-containing tripodal ligand. *RSC Adv.* **2015**, *5*, 10521–10528.
- (54) Palepu, N. R.; Nongbri, S. L.; Premkumar, J. R.; Verma, A. K.; Bhattacharjee, K.; Joshi, S. R.; Forbes, S.; Mozharivskyj, Y.; Thounaojam, R.; Aguan, K.; Kollipara, M. R. Synthesis and evaluation of new salicylaldehyde–2–picolinylhydrazone Schiff base compounds of Ru(II), Rh(III) and Ir(III) as in vitro antitumor, antibacterial and fluorescence imaging agents. *J. Biol. Inorg. Chem.* **2015**, *20*, 619–638.
- (55) Appelt, P.; Fagundes, F. D.; Facchin, G.; Kramer, M. G.; Back, D. F.; Cunha, M. A. A.; Sandrino, B.; Wohnrath, K.; de Araujo, M. P. Ruthenium(II) complexes containing 2-mercaptothiazolines as ligands and evaluation of their antimicrobial activity. *Inorg. Chim. Acta* **2015**, *436*, 152–158.
- (56) Sun, D.; Zhang, W.; Yang, E.; Li, N.; Liu, H.; Wang, W. Investigation of antibacterial activity and related mechanism of a ruthenium(II) polypyridyl complex. *Inorg. Chem. Commun.* **2015**, *56*, 17–21.
- (57) Chatterjee, D.; Banerjee, P.; Bose K, J. C.; Mukhopadhyay, S. Peroxydisulfate activation by  $[\text{Ru}^{\text{II}}(\text{tpy})(\text{pic})(\text{H}_2\text{O})]^+$ . Kinetic, mechanistic and anti-microbial activity studies. *Dalton Trans.* **2012**, *41*, 2694–2698.
- (58) Li, F.; Mulyana, Y.; Feterl, M.; Warner, J. M.; Collins, J. G.; Keene, F. R. The antimicrobial activity of inert oligonuclear polypyridylruthenium(II) complexes against pathogenic bacteria, including MRSA. *Dalton Trans.* **2011**, *40*, 5032–5038.
- (59) Pandrala, M.; Li, F.; Feterl, M.; Mulyana, Y.; Warner, J. M.; Wallace, L.; Keene, F. R.; Collins, J. G. Chlorido-containing ruthenium(II) and iridium(III) complexes as antimicrobial agents. *Dalton Trans.* **2013**, *42*, 4686–4694.

- (60) Li, F.; Feterl, M.; Warner, J. M.; Keene, F. R.; Collins, J. G. Dinuclear polypyridylruthenium(II) complexes: flow cytometry studies of their accumulation in bacteria and the effect on the bacterial membrane. *J. Antimicrob. Chemother.* **2013**, *68*, 2825–2833.
- (61) Gorle, A. K.; Li, X.; Primrose, S.; Li, F.; Feterl, M.; Kinobe, R. T.; Heimann, K.; Warner, J. M.; Keene, F. R.; Collins, J. G. Oligonuclear polypyridylruthenium(II) complexes: selectivity between bacteria and eukaryotic cells. *J. Antimicrob. Chemother.* **2016**, *71*, 1547–1555.
- (62) Karpin, G. W.; Morris, D. M.; Ngo, M. T.; Merola, J. S.; Falkinham III, J. O. Transition metal diamine complexes with antimicrobial activity against *Staphylococcus aureus* and methicillin-resistant *S. aureus* (MRSA). *Med. Chem. Commun.* **2015**, *6*, 1471–1478.
- (63) Pankey, G. A.; Sabath, L. D. Clinical relevance of bacteriostatic versus bactericidal mechanisms of action in the treatment of Gram-positive bacterial infections. *Clin. Infect. Dis.* **2004**, *38*, 864–870.
- (64) Lam, P. -L.; Lu, G. -L.; Hon, K. -M.; Lee, K. -W.; Ho, C. -L.; Wang, X.; Tang, J. C. -O.; Lam, K. -H.; Wong, R. S. -M.; Kok, S. H. -L.; Bian, Z. -X.; Li, H.; Lee, K. K. -H.; Gambari, R.; Chui, C. -H.; Wong, W. -Y. Development of ruthenium(II) complexes as topical antibiotics against methicillin resistant *Staphylococcus aureus*. *Dalton Trans.* **2014**, *43*, 3949–3957.
- (65) Nemeth, J.; Oesch, G.; Kuster, S. P. Bacteriostatic versus bactericidal antibiotics for patients with serious bacterial infections: systematic review and meta-analysis. *J. Antimicrob. Chemother.* **2015**, *70*, 382–395.
- (66) Romero-Canelón, I.; Salassa, L.; Sadler, P. J. The contrasting activity of iodo versus chlorido ruthenium and osmium arene azo- and imino-pyridine anticancer complexes: control of cell selectivity, cross-resistance, p53 dependence, and apoptosis pathway. *J. Med. Chem.* **2013**, *56*, 1291–1300.

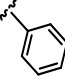
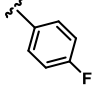
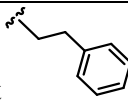
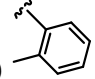
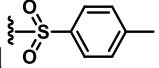
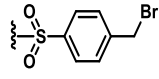
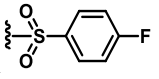
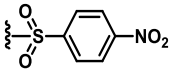
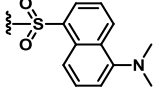
- (67) Dougan, S. J.; Habtemariam, A.; McHale, S. E.; Parsons, S.; Sadler, P. J.; Catalytic organometallic anticancer complexes. *Proc. Natl. Acad. Sci. U. S. A.* **2008**, *105*, 11628–11633.
- (68) Selbach, B.; Earles, E.; Dos Santos, P. C. Kinetic analysis of the bisubstrate cysteine desulfurase SufS from *Bacillus subtilis*. *Biochemistry* **2010**, *49*, 8794–8802.
- (69) VanDuinen, A. J.; Winchell, K. R.; Keithly, M. E.; Cook, P. D. X-ray crystallographic structure of BshC, a unique enzyme involved in Bacillithiol biosynthesis. *Biochemistry* **2015**, *54*, 100–103.
- (70) Finberg, R. W.; Moellering, R. C.; Tally, F. P.; Craig, W. A.; Pankey, G. A.; Dellinger, E. P.; West, M. A.; Joshi, M.; Linden, P. K.; Rolston, K. V.; Rotschafer, J. C.; Rybak, M. J. The importance of bactericidal drugs: future directions in infectious disease. *Clin. Infect. Dis.* **2004**, *39*, 1314–1320.
- (71) French, G. L. Bactericidal agents in the treatment of MRSA infections—the potential role of daptomycin. *J. Antimicrob. Chemother.* **2006**, *58*, 1107–1117.
- (72) Forbes, S.; Dobson, C. B.; Humphreys, G. J.; McBain, A. J. Transient and sustained bacterial adaptation following repeated sublethal exposure to microbicides and a novel human antimicrobial peptide. *Antimicrob. Agents Chemother.* **2014**, *58*, 5809–5817.
- (73) Castillo, J. A.; Clapés, P.; Infante, M. R.; Comas, J.; Manresa, Á. Comparative study of the antimicrobial activity of bis(N<sup>α</sup>-caproyl-L-arginine)-1,3-propanediamine dihydrochloride and chlorhexidine dihydrochloride against *Staphylococcus aureus* and *Escherichia coli*. *J. Antimicrob. Chemother.* **2006**, *57*, 691–698.
- (74) Chindera, K.; Mahato, M.; Sharma, A. K.; Horsley, H.; Kloc-Muniak, K.; Kamaruzzaman, N. F.; Kumar, S.; McFarlane, A.; Stach, J.; Bentin, T.; Good, L. The antimicrobial polymer PHMB enters cells and selectively condenses bacterial chromosomes. *Sci. Rep.* **2016**, *6*, 23121.
- (75) Sweeney, D.; Raymer, M. L.; Lockwood, T. D. Antidiabetic and antimalarial biguanide drugs are metal-interactive antiproteolytic agents. *Biochem. Pharmacol.* **2003**, *66*, 663–677.

- (76) Davidoff, F.; Carr, S. Calcium-like action of phenethylbiguanide and related compounds: inhibition of pyruvate kinase. *Proc. Natl. Acad. Sci. U.S.A.* **1972**, *69*, 1957-1961.
- (77) Veith, N.; Feldman-Salit, A.; Cojocaru, V.; Henrich, S.; Kummer, U.; Wade, R. C. Organism-adapted specificity of the allosteric regulation of pyruvate kinase in lactic acid bacteria. *PLOS Comput. Biol.* **2013**, *9*, e1003159.
- (78) Sheldrick, G. M. *SHELXT*—Integrated space-group and crystal structure determination. *Acta Cryst.* **2015**, *A71*, 3–8.
- (79) Sheldrick, G. M. A short history of *SHELX*. *Acta Cryst.* **2008**, *A64*, 112–122.
- (80) Pizarro, A. M.; McQuitty, R. J.; Mackay, F. S.; Zhao, Y.; Woods, J. A.; Sadler, P. J. Cellular accumulation, lipophilicity and photocytotoxicity of diazido platinum(IV) anticancer complexes. *ChemMedChem* **2014**, *9*, 1169–1175.
- (81) Clinical and Laboratory Standards Institute. *Performance standards for antimicrobial susceptibility testing; twenty-fifth informational supplement*. CLSI document M100-S25; Wayne, PA, 2015; Vol. 35.
- (82) Werthen, M.; Henriksson, L.; Jensen, P. O.; Sternberg, C.; Givskov, M.; Bjarnsholt, T. An *in vitro* model of bacterial infections in wounds and other soft tissues. *APMIS* **2010**, *118*, 156-164.
- (83) R Core Team. R: A language and environment for statistical computing. R foundation for statistical computing. **2016** Vienna, Austria. URL <https://www.R-project.org/>.
- (84) Lenth, R. V. Least-squares means: The R package lsmeans. *J. Stat. Softw.* **2016**, *69*, 1-33.

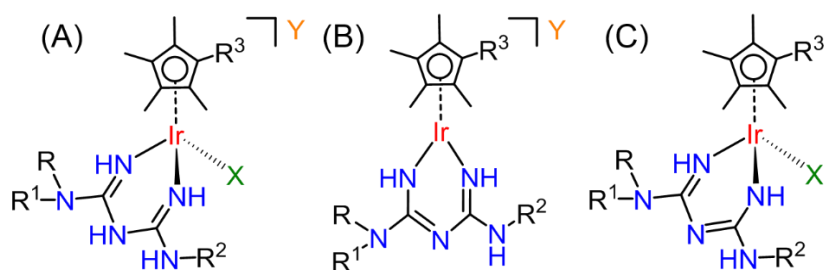
**Chart 1. Biguanide Ligands with Various Functional Substituents.**



**Biguanide**

Ligand	Name	R	R <sup>1</sup>	R <sup>2</sup>
<b>L1</b>	Metf	Me	Me	H
<b>L2</b>	PhBig	Phenyl 	H	H
<b>L3</b>	4-F-PhBig	4-F-phenyl 	H	H
<b>L4</b>	PhEtBig	PhEt 	H	H
<b>L5</b>	TolBig	1-(o-Tolyl) 	H	H
<b>L6</b>	TolSul-Big-Tol	1-(o-Tolyl)	H	TolSul 
<b>L7</b>	4-(BrCH <sub>2</sub> )-PhSul-Big-Tol	1-(o-Tolyl)	H	4-Br-PhSul 
<b>L8</b>	4-F-PhSul-Big-Tol	1-(o-Tolyl)	H	4-F-PhSul 
<b>L9</b>	4-NO <sub>2</sub> -PhSul-Big-Tol	1-(o-Tolyl)	H	4-NO <sub>2</sub> -PhSul 
<b>L10</b>	Dan-Big-Tol	1-(o-Tolyl)	H	Dan 

**Chart 2. Structures of Complexes 1-14 Studied in This Work**



Complex (struct type)	R <sup>3</sup>	X	Y	Big <sup>a</sup>
<b>1 (A)</b>	Me	Cl	Cl	<b>L1</b>
<b>2 (A)</b>	Ph	Cl	Cl	<b>L1</b>
<b>3 (A)</b>	Biph	Cl	Cl	<b>L1</b>
<b>4 (B)</b>	Biph	Cl	-	<b>L2-H</b>
<b>5 (B)</b>	Biph	Cl	-	<b>L3-H</b>
<b>6 (A)</b>	Biph	Cl	Cl	<b>L4</b>
<b>7 (A)</b>	Biph	Cl	Cl	<b>L4</b>
<b>8 (A)</b>	Biph	Br	Br	<b>L4</b>
<b>9 (A)</b>	Biph	I	I	<b>L5</b>
<b>10 (C)</b>	Biph	Cl	-	<b>L6-H</b>
<b>11 (C)</b>	Biph	Cl	-	<b>L7-H</b>
<b>12 (C)</b>	Biph	Cl	-	<b>L8-H</b>
<b>13 (C)</b>	Biph	Cl	-	<b>L9-H</b>
<b>14 (C)</b>	Biph	Cl	-	<b>L10-H</b>

<sup>a</sup>Biguanide ligands L1-L10, see Chart 1: in L, the biguanide is protonated on the backbone N; in L-H, biguanide is deprotonated.

**Table 1. Selected Bond Lengths (Å) and Angles (°) for Complexes 1 and 4**

Bonds	Bond Length (Å)/Angle (°)	
	<b>1</b>	<b>4</b>
Ir1-N <sup>a</sup>	2.087(2)	1.975(3)
Ir1-N <sup>b</sup>	2.074(2)	1.973(3)
Ir1-Cp <sup>x</sup> (Centroid)	1.777	1.775
C <sup>a</sup> -N <sup>a</sup>	1.287(4)	1.346(5)
C <sup>a</sup> -N <sup>c</sup>	1.382(4)	1.331(5)
C <sup>b</sup> -N <sup>b</sup>	1.301(4)	1.348(4)
C <sup>b</sup> -N <sup>c</sup>	1.382(4)	1.321(5)
N <sup>a</sup> -Ir1-N <sup>b</sup>	84.97(9)	85.38(13)
C <sup>a</sup> -N <sup>c</sup> -C <sup>b</sup>	124.3(2)	122.2(3)

N<sup>a</sup> corresponds to N5, N111; N<sup>b</sup>: N3, N108; N<sup>c</sup>: N4, N109  
C<sup>a</sup> corresponds to C5 C110; C<sup>b</sup>: C3, C108

**Table 2. Antibacterial Activity (MIC and MBC), Cytotoxicity (CC<sub>50</sub>), Haemolytic Activity (HC<sub>50</sub>), and Cytopathic Effect (IC<sub>50</sub>) of Complexes 1-14**

Complex	<i>S. aureus</i>	<i>B. subtilis</i>	<i>S. pyogenes</i>	<i>S. epidermidis</i>	<i>E. faecalis</i>	<i>HEK-293</i>	<i>RBC</i>	<i>HaCaT</i>
	Gram-positive bacteria <sup>a</sup> MIC/MBC (μg/mL) (MIC/MBC (μM))					Mammalian <sup>b</sup> μg/mL (μM)		
1	>32/>32 (>59.7)	>32/>32 (>59.7)	>32/>32 (>59.7)	>32/>32 (>59.7)	>32/>32 (>59.7)	>32 (>59.7)	n. d.	n. d.
2	>32/>32 (>54.3)	>32/>32 (>54.3)	>32/>32 (>54.3)	>32/>32 (>54.3)	>32/>32 (>54.3)	>32 (>54.3)	n. d.	n. d.
3	8/8 (12.6)	4/4 (6.3)	2/2 (3.2)	4/16 (6.3/25)	8/32 (12.6/50)	27.4 (43.5)	n. d.	n. d.
4	2/2 (2.9)	0.5/0.5 (0.7)	0.25/1 (0.4/1.5)	0.25/0.5 (0.4/0.7)	1/8 (1.5/11.7)	>32 (>47)	6.1 (9.0)	64 (94)
5	2/2 (2.8)	0.5/0.5 (0.7)	0.25/0.25 (0.4)	0.5/0.5 (0.7)	1/8 (1.4/11.2)	>32 (>45)	11.8 (16.9)	128 (179)
6	2/2 (2.7)	1/2 (1.3/2.7)	0.125/0.5 (0.17/0.7)	0.25/0.25 (0.3)	1/32 (1.3/43.1)	17.2 (23.2)	21 (28.3)	128 (173)
7	1/2 (1.4/2.8)	0.25/0.5 (0.3/0.7)	0.125/0.125 (0.17)	0.5/0.5 (0.7)	1/4 (1.4/5.6)	>32 (>44)	14.6 (20)	128 (176)
8	0.5/1 (0.6/1.2)	0.5/1 (0.6/1.2)	0.25/0.25 (0.3)	0.5/1 (0.6/1.2)	0.5/32 (0.6/37)	23.7 (27.6)	6.7 (8.2)	n. d.
9	0.5/4 (0.5/4.4)	0.25/1 (0.3/1.1)	0.25/0.25 (0.3)	0.5/0.5 (0.5)	1/16 (1.1/17.6)	17.0 (18.6)	7.8 (8.6)	n. d.
10	0.5/>32 (0.6/>38)	0.5/16 (0.6/19)	0.25/0.25 (0.3)	0.25/>32 (0.3/>38)	>32/>32 (>38)	>32 (>38)	14.6 (17)	n. d.
11	0.5/>32 (0.5/>35)	0.5/16 (0.5/17)	1/2 (1.1/2.2)	0.5/>32 (0.5/>35)	>32/>32 (>35)	>32 (>35)	>32 (>35)	128 (139)
12	0.5/>32 (0.6/>38)	1/32 (1.2/38)	1/8 (1.2/9.4)	0.25/>32 (0.3/>38)	>32/>32 (>38)	>32 (>38)	>32 (>38)	128 (151)
13	0.5/>32 (0.6/>38)	0.5/16 (0.6/19)	0.5/8 (0.6/9.5)	0.25/>32 (0.3/>38)	>32/>32 (>38)	>32 (>38)	25 (30)	n. d.
14	0.5/>32 (0.5/>35)	0.5/32 (0.5/35)	1/4 (1.1/4.4)	0.25/>32 (0.3/>35)	>32/>32 (>35)	>32 (>35)	>32 (>35)	32 (35)
Van	2/>32 (1.4/>22)	0.25/0.25 (0.2)	1/1 (0.7)	4/4 (2.8)	4/>32 (2.8/>22)	n. d.	n. d.	n. d.

<sup>a</sup>Bacterial strains: *S. aureus*, ATCC 29213; *B. subtilis*, DSM 10; *S. pyogenes*, ATCC 151112; *S. epidermidis*, ATCC 12228; *E. faecalis*, ATCC 29212. <sup>b</sup>Mammalian cells: *HEK-293* human embryonic kidney cells ATCC CRL-1573 (CC<sub>50</sub>), *RBC* human red blood cells (HC<sub>50</sub>), *HaCaT* human keratinocytes cells (IC<sub>50</sub>).



**Table 3. Effect of Complexes 4, 7 and 10 on the Activity of Cefoxitin (Cef) and Vancomycin (Van) towards MRSA and VRE (MIC µg/mL)**

Strain	Cef	Van	<b>4</b>			<b>7</b>			<b>10</b>		
			<b>4</b>	<b>4+Cef</b>	<b>4+Van</b>	<b>7</b>	<b>7+Cef</b>	<b>7+Van</b>	<b>10</b>	<b>10+Cef</b>	<b>10+Van</b>
MRSA	32	n.d.	2	32	n. d.	0.5	32	n. d.	0.5	32	n. d.
VRE	n.d.	64	4	n. d.	0.25	2	n. d.	4	4	n. d.	2

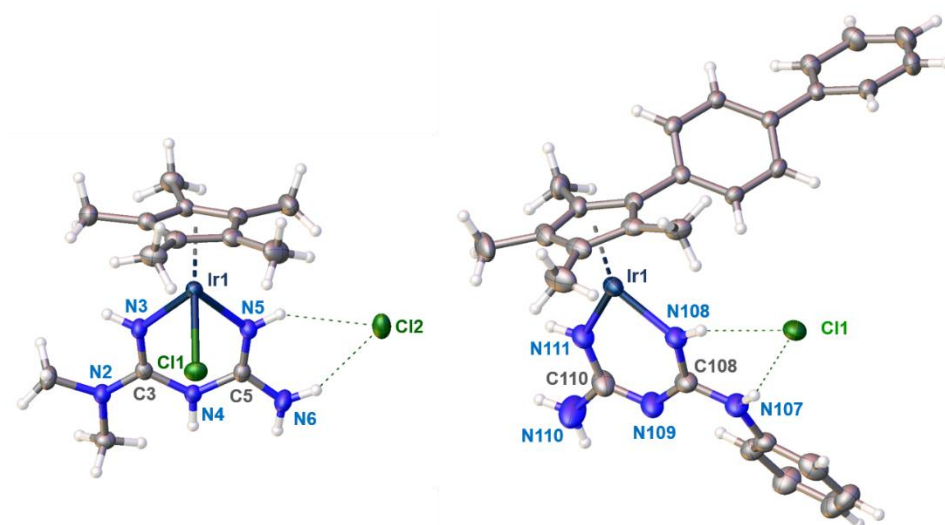


**Figure 1.** Structures of Ir<sup>III</sup> complexes **1** (left) and **4** (right) and with atom labelling. Thermal ellipsoids are drawn at 50% probability level.

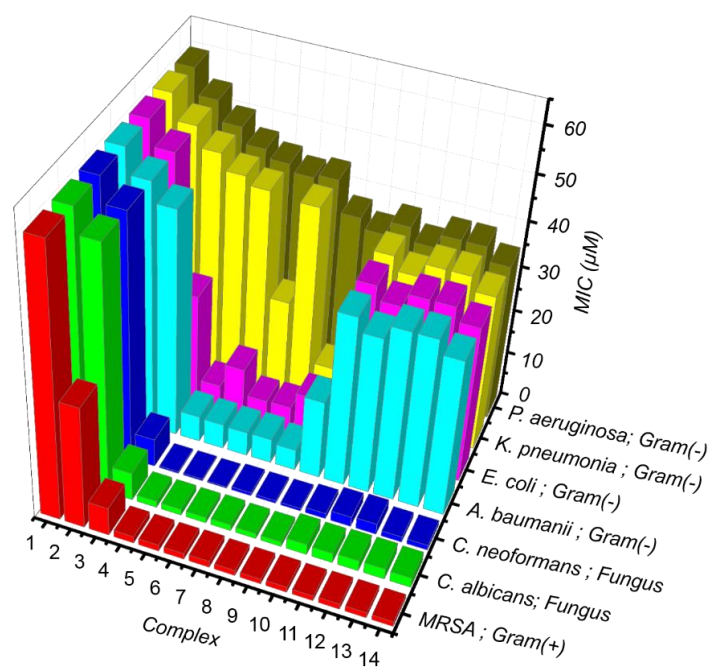


**Figure 2.** Selected antimicrobial data of complexes **1-14**, as MIC values in  $\mu\text{M}$ . Bacterial strain types: *A. baumannii*: ATCC 19606; *E. coli*: ATCC 25922; *K. pneumoniae*: ATCC 700603; MRSA: ATCC 43300; *C. albicans*: ATCC 90028; *C. neoformans*: ATCC 208821. Further activity data for these complexes are listed in Table S4.

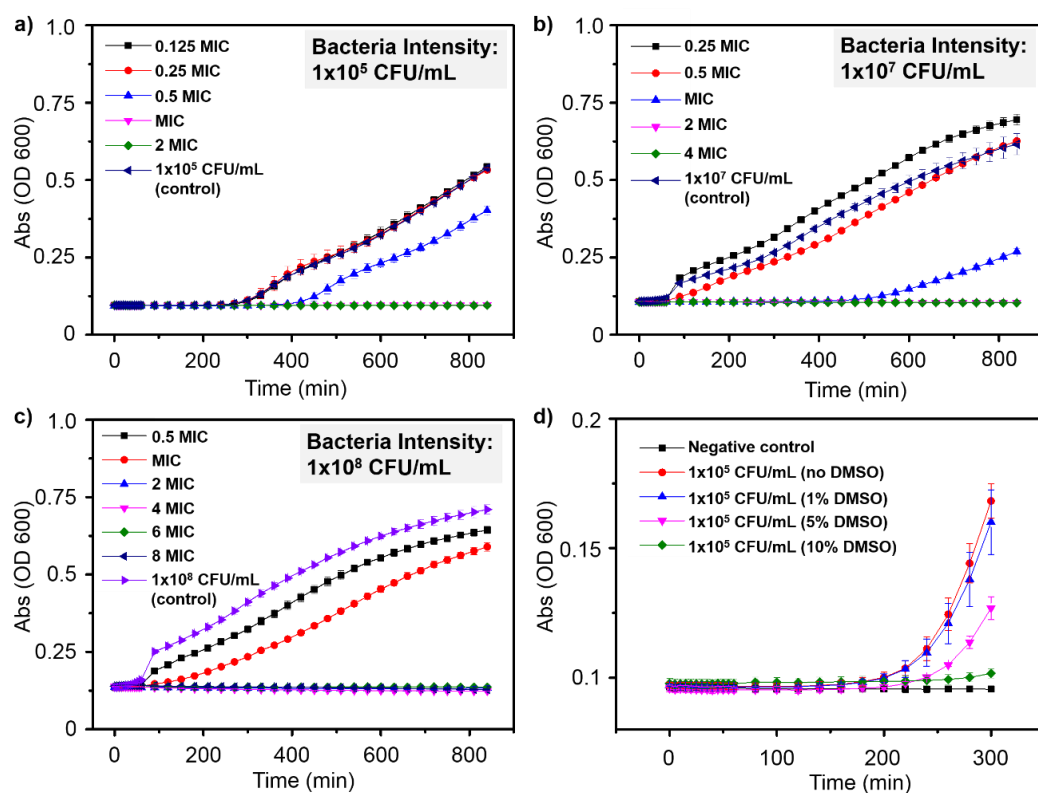


**Figure 3.** Kinetics of growth inhibition for complex 7 against *S. aureus*, a) bacterial suspension of  $1 \times 10^5$  CFU/mL with complex concentrations ranging from 0.125 MIC to 2 MIC; b) bacterial suspension of  $1 \times 10^7$  CFU/mL with complex concentrations from 0.25 MIC to 4 MIC; c) bacterial suspension of  $1 \times 10^8$  CFU/mL with complex concentrations from 0.5 MIC to 8 MIC; d) effect of DMSO on the growth of bacteria.

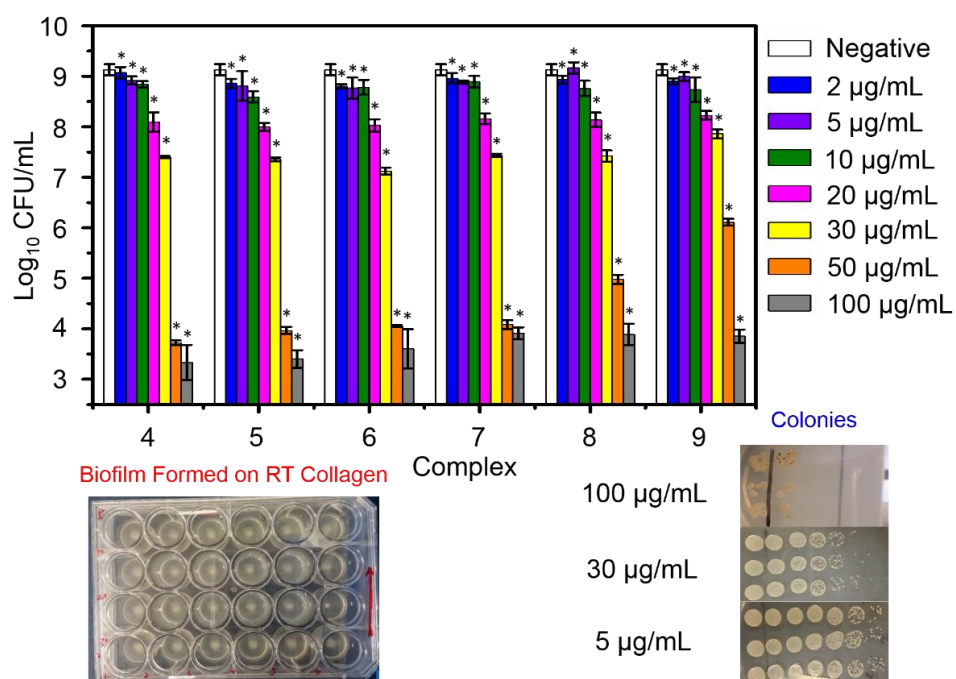


**Figure 4.** *S. aureus* biofilm disruption of complexes 4-9 at a variety of complex concentrations indicated as logarithm of the number of bacteria. Analysis of variance (ANOVA) determined that both complex and concentration had an effect on number of viable bacteria; post-hoc comparison of each treatment with the negative control (bacterial culture without any antibiotics) showed that all complexes killed bacteria, even at the lowest concentration tested ( $p < 0.05$  for \*).

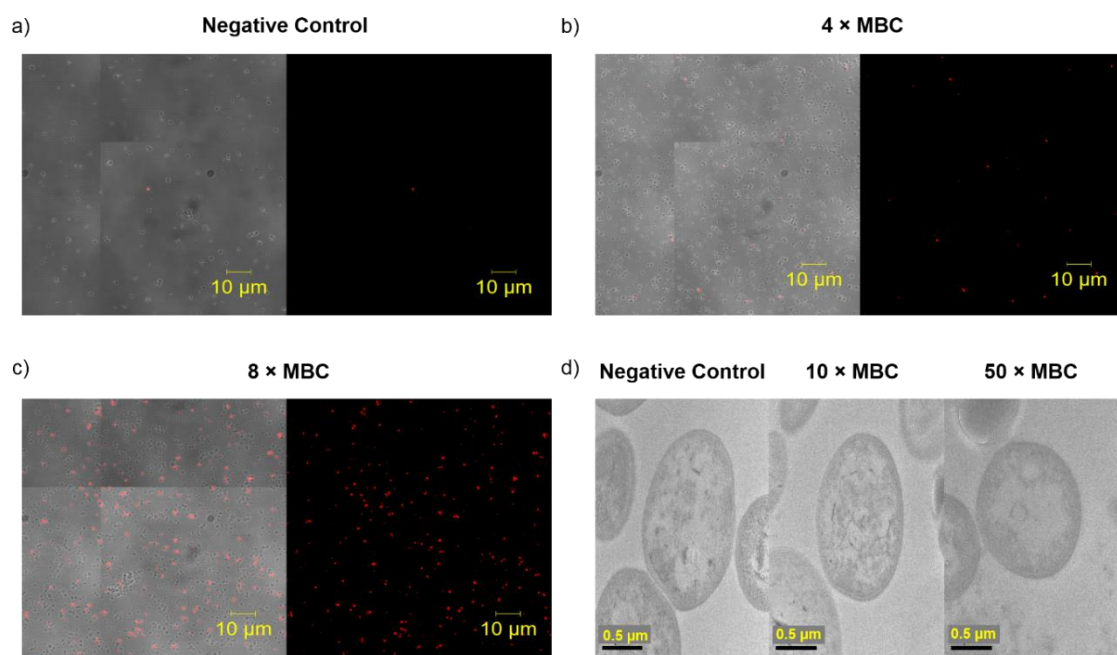


**Figure 5.** Monitoring of the permeability change of cell membranes of *S. aureus* (ATCC 29213) induced by complex **7** via PI staining and confocal microscopy, and morphological changes by TEM; a-c) complex **7** at concentrations of 0, 4 $\times$  MBC and 8 $\times$  MBC, respectively; the left images show the contrast mode of both stained and unstained cells and the right images suggest the PI fluorescence cells; d) TEM images, treatment of complex **7** at concentrations of 10 $\times$  MBC (left) and 50 $\times$  MBC (right).